ABSTRACT

COMBINED EFFECTS OF PROZAC AND HYPOTHALAMIC MEDIATED RESPONSE ON MASSETER MUSCLE ACTIVITY IN THE CAT

by

Chika P. Nwaorgu

The present study tested the hypothesis that infusion of Prozac would serve to suppress defensive rage elicited from the medial hypothalamus of the cat. Cats are known to exhibit certain kind of behavior, known as the "defensive rage response" such as unsheathing of the claws, retraction of the ear and vocalization (hissing).

Three adult cats (2 males and 1 female) weighing (2.8 – 3.4 kg) were utilized during the experiments. Cannula-electrodes were implanted into the medial hypothalamus for elicitation of defensive rage behavior. EMG activity was recorded with a bipolar electrode attached to the masseter muscle to establish baseline before the infusion of the drug. Mean frequency values of early and late stimulation were calculated using the continuous wavelet transform.

The effects of early stimulation of the medial hypothalamus upon response latencies were compared with those of the late stimulation. The results reveal an inhibitory effect that may be related to fatigue or other inhibitory structures in the brain. The mean frequency values of the early stimulation on average were significantly higher than the mean frequency values of the late stimulation ($p = 0.03$). While baseline (pre-injection) mean values among the three subjects during early and late stimulation were highly significant ($p = 0.003$), there were no significant differences among post-injection mean values ($p > 0.05$). The findings suggest that infusion of the drug has some inhibitory influence on the masseteric EMG activity.

COMBINED EFFECTS OF PROZAC AND HYPOTHALAMIC MEDIATED RESPONSE ON MASSETER MUSCLE ACTIVITY IN THE CAT

by
Chika P. Nwaorgu

A Thesis
Submitted to the Faculty of
New Jersey Institute of Technology
In Partial Fulfillment of the Requirements for the Degree of
Master of Science in Biomedical Engineering

Department of Biomedical Engineering

August 2005

APPROVAL PAGE

COMBINED EFFECTS OF PROZAC AND HYPOTHALAMIC MEDIATED RESPONSE ON MASSETER MUSCLE ACTIVITY IN THE CAT

Chika P. Nwaorgu

Dr. Stanley S. Reisman, Thesis Advisor — Date
Professor of Biomedical Engineering, NJIT
Professor of Electrical and Computer Engineering, NJIT

Dr. Ronald H. Rockland, Committee Member — Date
Associate Professor of Engineering Technology and Biomedical Engineering, NJIT

Dr. Saul Weiner, Committee Member — Date
Professor of Prosthodontics and Biomaterials, UMDNJ

BIOGRAPHICAL SKETCH

Author: Chika P. Nwaorgu

Degree: Master of Science

Date: August 2005

Undergraduate and Graduate Education:

- Master of Science in Biomedical Engineering
  New Jersey Institute of Technology, Newark, NJ, 2005

- Bachelor of Science in Computer Science
  New Jersey Institute of Technology, Newark, NJ, 2000

Major: Biomedical Engineering

This thesis is dedicated to

my beloved mother, Teresa Mmaku Nwaorgu, who supported me with her powerful prayers, and to Jean Perkins, for her unconditional support and encouragement.

ACKNOWLEDGMENT

The author wishes to express his genuine gratitude to his advisor, Dr. Stanley Reisman, for his guidance and patience throughout this research.

Special thanks to Dr. Weiner not only for serving as a member of the committee, but also for his immense contribution to this research. The author owes thanks as well to a truly good friend, Frank Tom Jr., for his kindness and unwavering support.

Finally, the author wishes to give his deepest thanks to his brother, Rev. Fr. Anselm Nwaorgu, who has been there for him when it counts the most.

TABLE OF CONTENTS

TABLE OF CONTENTS
(Continued)

Chapter **Page**

LIST OF TABLES

LIST OF FIGURES

LIST OF FIGURES
(Continued)

CHAPTER 1

BACKGROUND

1.1 Introduction

Muscloskeletal disorders are a significant health problem in the United States. These disorders are poorly understood in spite of their wide0spread prevalence. However, it is commonly accepted that there are two components represented in these disorders: a muscular dysfunction component and an emotional component. Because of the complexity of these disorders, an experimental model may prove useful. In the cat, electrical stimulation of sites in the hypothalamus from which emotional behaviors can be elicited appears to be a useful model for analysis of these conditions. The emotional behaviors are standardized and changes resulting from experimental manipulation can be quantified. This experimental model has been utilized in several studies that have compared jaw motor responses during mastication verses emotional behavior and the effects of pharmacologic agents known to modulate emotional responses. These proposed experiments would extend the previous observations by utilizing an SSRI, which potentiates the effects of serotonin, a neurotransmitter important in the mediation of emotional behavior and mood. Its effects upon hypothalamic modulation of masseteric activity were the basis for this study.

The traditionally used methods for the analysis of surface electromyography (SEMG) signals are the fast Fourier transform (FFT) and the short-time Fourier transform (STFT). However they both suffer from limitations. For instance, they are only suitable for stationary signals. However, even when there is no voluntary change of muscle state, EMG signals are non-stationary due to the physiology of the system (i.e. variance in

blood flow). This suggests that these traditional methods are not the appropriate approaches for the analysis of signals with transient components in time such as the SEMG signal. A relatively new technique, the wavelet transform, is well suited to nonstationary signals, and overcomes the limitations of the traditional time-frequency methods. Wavelets are a new powerful tool for signal processing that act as a "microscope" in which one can observe different parts of the signal by adjusting the focus. This allows the detection of short-lived time components of the signal. In the wavelet transform the signal is decomposed into elementary components well localized in the time domain and in the frequency domain. The wavelet transform provides insight into the structure of the time series at various scales. It allows localizing changes of the signal in time, providing additional information in comparison with the Fourier transform. This method has been successfully used in analyzing a number of biomedical signals such as heart rate variability, EEG signals, and electromyographic (EMG) signals.

The amplitude and frequency responses of the electromyographic signal indicate the activation level within the muscle. The force achieved by the muscle depends on the activation level, the number and fiber type of the muscle fibers activated, the contraction dynamics, and the history of previous contractions. Fast- and slow-twitch muscle fibers have different intrinsic contraction properties [16], and it is typically thought that slow-twitch fibers are recruited for low-intensity activities, with a greater proportion of fast-twitch fibers being recruited as increasing force is required [17]. The frequency components of the EMG signal can indicate the muscle fiber type recruitment for any given activity. The frequency increases with greater conduction velocities of the muscle fiber action potentials [18]. Action potentials travel faster along larger-diameter cells.

Muscle fiber recruitment strategies can thus be determined from the EMG frequency spectra, and this has previously been demonstrated for graded muscle contractions in the cat gastrocnemius [19]. The timing, activation level, and motor unit recruitment patterns leave characteristic features within the EMG signal. The ability to resolve time, intensity, and frequency simultaneously gives insight into the muscles recruitment pattern.

This research employed the wavelet transform, also known as multi-resolution analysis, to the masseteric surface EMG recorded experimentally. These analyses gave a clearer understanding of the nature of hypothalamic modulation of jaw muscle activity during emotional state.

1.2 Hypothesis

The first aspect of our hypothesis is that infusion of SSRI will affect the hypothalamic-elicited behavior in a time dependent spectral shift observed in the masseteric EMG either upwards or downwards. The second aspect of the hypothesis states that after one hour of infusion of SSRI, the observed spectral distribution of the masseteric EMG is reversed.

1.3 Physiological Research

The changes in muscle function associated with neuromuscular disorders are poorly understood. While a number of studies have demonstrated increased muscle activity associated with anxiety and emotional behavior [4], the relationship between such changes in muscle activity and neuromuscular disorders are not well defined. A significant issue in understanding the pathogenesis of these disorders is the

characterization of the EMG signal. Using the cat model, there were shifts in frequency of contraction for muscle fibers associated with expression of hypothalamically-elicited emotional behavior. The masseter muscle, responsible for jaw movement, demonstrates an upward shift in frequency during the elicitation of this aggressive behavior in a time-dependent spectral analysis [4].

1.3.1 Expression of Emotional Behaviors

The cat is an excellent model to study the interaction between emotional responses and muscle activity because patterned emotional responses can be readily elicited. These include defensive rage (affective defense) behavior or predatory attack (quiet biting attack) behavior.

1.3.2 Defensive Rage Behavior

Defensive rage behavior in the cat is characterized by various sympathetic signs, such as pupillary dilation, piloerection, ear retraction, salivation, unsheathing of the claws, hissing and paw strike [5]. This behavior occurs under both natural and experimental laboratory conditions. Naturally, it occurs in a variety of situations, which are perceived as threatening to the animal. For example, this response may occur when a cat perceives that her kittens are endangered by another animal, or when a cat's territory is invaded. In the laboratory, it can be reliably elicited by electrical stimulation of the medial hypothalamus or the midbrain periaqueductal gray (PAG). The dependent variable often measured by experimenters is the time between stimulation onset and onset of the audible portion of the hiss response. This response typically involves mouth opening and then a

hiss [6, 7]. It should be noted that the stimulation applied at medial hypothalamic sites from which defensive rage can be elicited produces marked increases in heart rate, blood pressure, and peripheral epinephrine and norepinephrine levels [8].

1.3.3 Predatory attack behavior

Predatory attack is defined as occurring when the cat bites the target. Quiet biting attack behavior, which is predatory in nature, is typically characterized by "stalking" of a prey such as an anesthetized rat, followed by the biting of the back of it neck. The attack begins after onset of stimulation and usually persists until stimulation is terminated. Occasionally, the cat may also strike its prey with its forepaw prior to biting it [9]. This behavior is similar to the response that occurs under natural conditions where stalking and killing of a rat is readily observed [5].

1.3.4 Advantages of the two Behavioral Models

The advantages of utilizing these models of aggression include: (1) they mimic closely the behavioral patterns displayed by cats under natural conditions; (2) the hypothalamic or PAG induced response can be elicited readily over many trials on a given experimental day. These responses can also be observed over subsequent daily sessions, enabling an investigator to examine the effects of such perturbations of the brain as experimental lesions and drug administration upon defensive rage and predatory attack behavior; as well as identify the functional anatomical circuits and their neurotransmitter systems that mediate the expression and modulation of these forms of aggressive behavior [10].

1.4 Selective Serotonin Re-uptake Inhibitors

Serotonin is a neurotransmitter that significantly influences aggressive behavior. In humans and in nonhuman primates decreased serotonin function is associated with violent or aggressive behavior [11]. In wild rats [12], serotonin concentrations in several brain regions were found to be higher in nonaggressive animals than in aggressive animals. In other laboratory animals, treatments that decrease serotonin function increase aggressive behavior, whereas treatments that increase serotonin function decrease aggressive behavior. In laboratory animal studies, drugs that increase serotonin function directly, by activating serotonin receptors, or indirectly, by increasing serotonin availability, reduce aggressive behavior [13]. In fact, there is evidence that activation of serotonin receptors in the medial hypothalamus can suppress rage behavior in the cat [14]. When viewed collectively, activation of serotonin receptors at both the levels of the hypothalamus as well as the PAG modulate defensive rage behavior.

Four types of SSRIs can be distinguished: fluoxetine (prozac), fluvoxamine, paroxetine, and sertraline. These are second and third generation antidepressants that enhance serotonin neurotransmission. Furthermore, studies of emotional and aggressive behavior, where motor activity has been monitored, have shown a link between expression of emotional affect and increases in muscle tension [4]. These findings are important in that they suggest that neuromuscular disorders have a component that may be related to emotionally-mediated motor activity. In the analysis phase of this research study, the effects of IV infusion of an SSRI antidepressant agent upon masseteric EMG activity generated by the stimulation of a predefined site in the hypothalamus were examined. The aim of this study was to evaluate wavelet transforms applications in the

analysis of masseter muscle contractility in cat subjects during stimulation of a certain region of the hypothalamus before and after the infusion of SSRI.

1.5 Stress and the Stress Response

It is important to have a clear understanding of the term stress in the context of this project. In this research, the term stress response refers to the physiological reaction of an animal or human to changes in its environment, such as the release of CRH (Corticotropin-releasing hormone) and oxytocin. Stressors are the stimuli that create the stress response. These stressors can be any or a combination of a variety of events, such as a change in temperature or the anticipation of a mental stress, such as an exam [22].

The stress response, initiated in the hypothalamus, is thought to modulate the muscle activation pathway followed during voluntary muscle activity. The planning and control of ongoing voluntary movements is dictated primarily by the cerebral cortex and cerebellum, and through interactions between the structures beneath the cortex, referred to as subcortical nuclei, and the cortex. This pathway that controls voluntary activity of the masseter muscle is also active during stress. However, the stress response that is initiated during hypothalamic stimulation interacts with this pathway to modulate the muscle activity. It is unclear how this modulation occurs during the stress response.

1.6 Skeletal Muscle and Electromyography

Contraction of skeletal muscles is accomplished through central nervous system interaction with motor nerve fibers, which innervate muscle fibers. A motor unit consists of a motoneuron and the muscle fibers that it innervates. Impulses are generated in the

motoneuron and propagate to the fibers of the motor unit. It has been observed that force of contraction is related to the frequency of the action potential and the number of motor units that are recruited [23]. Measurements of the electrical events associated with muscle contractions are known as electromyographic (EMG) recordings. These measurements give insight into the activation, or recruitment, pattern of the muscle. For instance, fast firing muscles display higher frequency content in the EMG recordings, whereas slow firing muscles display lower frequency content in the signal. Patterns of high and low frequency components in the signal indicate the recruitment pattern of the various types of muscle fibers during a contraction, as well as provide indications of fatigue [24, 25]. Fatigue has been measured, in purely frequency analyses, as the point at which the median frequency decreases. Dolan, et al. suggest that the increase in power in the low frequency range (5 – 30 Hz) has been found to be a more precise method of detecting muscle fatigue [25].

A muscle fiber "twitch" is defined as the mechanical response of a single fiber to a single action potential. There is a delay between the time when the electrical impulse stimulates the muscle fiber and the mechanical contraction of the muscle fiber. Once initiated, the mechanical contraction, or "twitch," may last up to 200 ms, while the action potential may last only 1-2 ms. The difference in reaction times enables the motoneuron to initiate a second impulse before the mechanical response to the first impulse has ended. This addition of electrical impulse before the mechanical activity has completed is known as summation as shown in figure 1.1. This results in a higher muscle tension during the time period that the electrical stimuli occur before the mechanical response of the fiber has ended.

This summation of fiber activity has a saturation point. This is the point at which increased frequency of the action potential relative to the duration of the muscle twitch will no longer cause an increase in tension. Rather, the muscle reaches a saturation point which varies depending upon whether the fiber is fast or slow firing, as well as upon the diameter of the fiber itself [26].

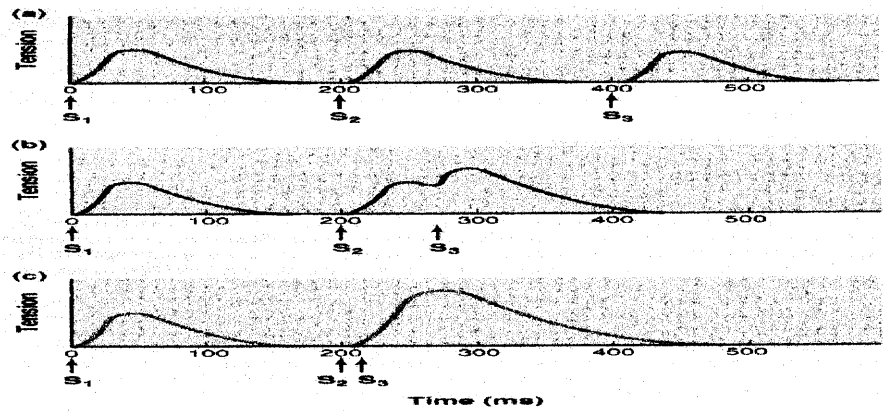

Figure 1.1 Summation of action potentials. Illustration of potentials that occur before the muscle twitch has ended and the resultant summation of muscle tension. S_1 and S_2 are the two stimuli. Note the increase in tension as the time between stimuli decreases.

An electrode placed parallel to the muscle of interest can detect the electrical impulses present during the muscle twitch. These potentials can be positive or negative, and as a result, the electromyographic signals captured during muscle activation contain both positive and negative, or polarized, components at any point in time. The recorded response of a motor unit has an amplitude of 0.1 – 5 mV. The frequencies present in EMG signals typically have a range from DC to 10 kHz, depending upon the diameter and type of muscle fiber that is being measured [27]. In this study, the data files were band passed from 2 to 750 Hz to remove DC voltage and to avoid any biasing effects. A biasing effect occurs when the sampling frequency is too low for the largest frequency

content in the signal. The Nyquist sampling theorem states that in order to avoid biasing effects in the signal, the sampling frequency must be at least twice as large as the highest frequency component (F_{max}) contained in the signal. In this case, the largest frequency component allowed to pass through the filter is 750 Hz. The signal was sampled at 2000 Hz, well over the $2*F_{max}$ (in this case after filtering, equivalent to 1500 Hz) limit imposed by the Nyquist sampling theorem. The data files were further notch filtered from 57.5 to 65 Hz to remove any 60 Hz or stimulation artifacts that may have been introduced into the recordings. The program that performed the filtering is written in Labview version 5.1. Both the front and wiring panels of the filtering program are included in Appendix A.

CHAPTER 2

EXPERIMENTAL PROCEDURES AND METHODS

This chapter describes the experimental setup and procedures for acquiring data and signal processing tools used for the analysis of the time and frequency components of the EMG signal. The data used in this experiment were obtained at the Limbic Research Laboratory at the Department of Neurosciences, New Jersey Medical School in Newark, New Jersey.

2.1 Preliminary Experiment and Data Analysis

The myoelectric activity detected with surface electrodes (SEMG) is the summation of the electrical signals generated by a number of motor units, active within the same motor territory in the proximity of the electrodes. The SEMG signal is a convenient parameter to studying the muscle behavior under fatiguing exercise, as it proves time-dependent changes, provided care is taken to prevent cross talk from adjacent muscles. The following subsections of (2.1) describe the methods and the results obtained in the preliminary experiment that was conducted as part of this research using a human subject.

A preliminary study was conducted as part of this research to address some of the engineering concerns such as the comparison of the Fast Fourier Transform (FFT) to the Continuous Wavelet Transform (CWT) using the mean power frequency parameter in analyzing the muscle fatigue, aiming to appreciate whether the CWT alone may be used to analyze the muscle behavior under fatiguing contraction. We are hypothesizing in this preliminary experiment that CWT can indicate the degree of muscle activation and

therefore can be used to analyze the development of muscle fatigue in the same way the FFT has been proved to do. The rationale for this study is that some of the parameters used to analyze fatigue indices using FFT approach may be comparable to the frequency responses of an emotionally stimulated muscle that is infused with SSRI.

The procedure to obtain the intensity from the measured EMG signal consisted of the following three major steps: (1) compute the continuous wavelet-transformed signal using daubechies 6 "db6"; (2) compute the square of the wavelet coefficients which is analogous to the power of the signal in Fourier transform [1], and (3) calculate the mean frequency in both the FFT and CWT using the formula

$MF = \sum C_i^2 * F_i / \sum F_i$

Where

MF = mean frequency

C = wavelet coefficients

F = frequencies derived from the scale

i = magnitude of the scale at the i^{th} position

2.1.1 Methods

One healthy male human subject participated with his consent. A pair of surface EMG self adhesive conductive gel electrodes (22.5 * 22.5 mm H59P, MVAP, USA), with their centers 25 mm apart from each other were placed on clean skin, longitudinally, immediately under the thickest point of the brachioradialis muscle of the left arm; a third similar electrode was placed on the branchioradialis muscle of the right arm to reduce noise interference. The task involved a steady isometric contraction, the subject standing

in an upright position, having to carry a weight on his left palm. In order to avoid movement artifact, the subject was asked to remain still through out the duration of the exercise. Visual feedback was used to insure the position of the hand was stationary during the task. The 100 % MVC was estimated at first for the subject under test, as the maximum weight that the subject could sustain for two seconds, after a few short preliminary trials for learning and breaks between trials to avoid fatigue. Two tests were performed for 25% MVC up to exhaustion.

Before acquiring data it was required to create files of appropriate size for data storage. The size of file was calculated using the sampling rate (S) per channel, the number of channels to be acquired (C), and the total sampling time (T).

Size = S*C*T (KB)

Size = 2000*1*90 = 180000 bytes

The SEMG signals were amplified (* 2000, Grass Model 79, USA) and acquired via a computerized acquisition system (CB68LP National Instrument, Labview 5.1, USA), at 2000 Hz sampling rate on one channel. All the programs for signal processing were written in MATLAB (MathWorks, Inc, USA) in conjunction with Wavelet Toolbox.

2.1.2 Results

The PSD spectra evolution computed on successive 5 s signal segments from SEMG, show compression toward lower frequencies with increasing fatigue both for the FFT and the CWT, starting at the very beginning of the contraction. The MF evolution shows a

progressive decrease from the very beginning of the task in both transforms. The similar evolutions of both the FFT and CWT support our hypothesis that CWT also indicates the degree of muscle activation and can be used to analyze the development of muscle fatigue.

For the subject, the linear regression was performed on the MF evolution to compute the slope, intercept, and correlation coefficient parameters.

FFT results:

Slope = -0.2135

Intercept = 182.5477

Correlation coefficient = -0.9315

CWT results:

Slope = -0.094

Intercept = 150

Correlation coefficient = -0.7862

In both cases (FFT and CWT) the linear regression slope of the MF evolution is negative. This implies that MF decreases from the very beginning of the muscle contraction. It also shows the central intervention in modulating the activation with increasing fatigue. The high negative correlation coefficient in both cases shows that the mean frequency, which is a principle parameter in the comparison decreases with time in both methods. While the correlation coefficient in the FFT method is higher than that of the CWT method, the difference may be explained by the fact that the CWT might provide different slopes in different sections of the signal due to mean frequency variations and therefore, a straight line fit might not be the most appropriate fit. Another factor could be because the mean

frequencies were averaged in 5-second blocks and concatenated over time due to large variations using the CWT method, which does not use all of the potential of the CWT.

The above discussion shows the intimate link between the FFT and the CWT (although averaging was used) as functionally related methods for analyzing SEMG. This study addresses a quantitative comparison (MF) of FFT and CWT. It brings additional evidence on the peripheral fatigue and provides means of quantifying the fatigue development in the isometric exercise. According to this study, the CWT can be used for analyzing the degree of muscle activation and for monitoring the muscle fatigue development in the isometric contraction. These observations provided the basis for the present study, which attempts to characterize the role of SSRI in modulating the frequency response of the masseter muscle elicited from the medial hypothalamus.

2.2 Subject Preparation

Three adult cats (2 males and 1 female) weighing (2.8 – 3.4 kg) were utilized in the experiments. The cats were individually housed throughout the course of all experiments. During aseptic surgery, the animals were deeply anesthetized with Isoflurane (1- 2%). 6 holes were drilled in the skull overlying both sides of the medial hypothalamus, lateral hypothalamus and the PAG, and stainless steel guide tubes were stereotaxically implanted over those holes with dental acrylic. Three stainless steel stylets connected to screws with silver wire were embedded in the skull and served as ground electrodes. Additionally, three bolts were anchored to the skull with dental acrylic and were attached to a plastic cap that protected the entire assembly.

2.3 Elicitation of Behavioral Response

Following surgery, the freely moving cat was placed in a wooden observation chamber (61 x 61 x 61 cm) with a clear Plexiglas door. Cannula electrodes were lowered vertically through guide tubes into the PAG sites from which defensive rage behavior could be elicited by electrical stimulation. Monopolar and cannula electrodes were lowered into the medial hypothalamus and electrical stimulation was applied at 0.5 mm steps in order to identify the sites from which defensive rage behavior could be elicited in the moving cat. When defensive rage behavior was reliably elicited from the medial hypothalamus within 15 s, the electrode was cemented in place with dental acrylic. The stimulating current ranged from 0.3-0.6 mA, 20 Hz, 0.05s per cycle duration. The peak-to-peak current was monitored by a Tektronix 5000 series oscilloscope.

2.4 Defensive Rage Behavior Elicited from the Medial Hypothalamus and the PAG.

The descending fibers from the rostral half of the medial hypothalamus to the dorsal part of the PAG has been considered as the principal pathway for the expression of defensive rage behavior [28]. Accordingly, in this study, defensive rage was elicited from the medial hypothalamus and the PAG as shown in figure 2.1, and Prozac was injected intraperitoneally (IP) into the stomach. This procedure permitted analysis of the role of Prozac receptors in the medial hypothalamus and PAG in modulating defensive rage. The use of this form of aggressive behavior also served as a behavioral control against possible non-specific sensory and motor effects of the drug.

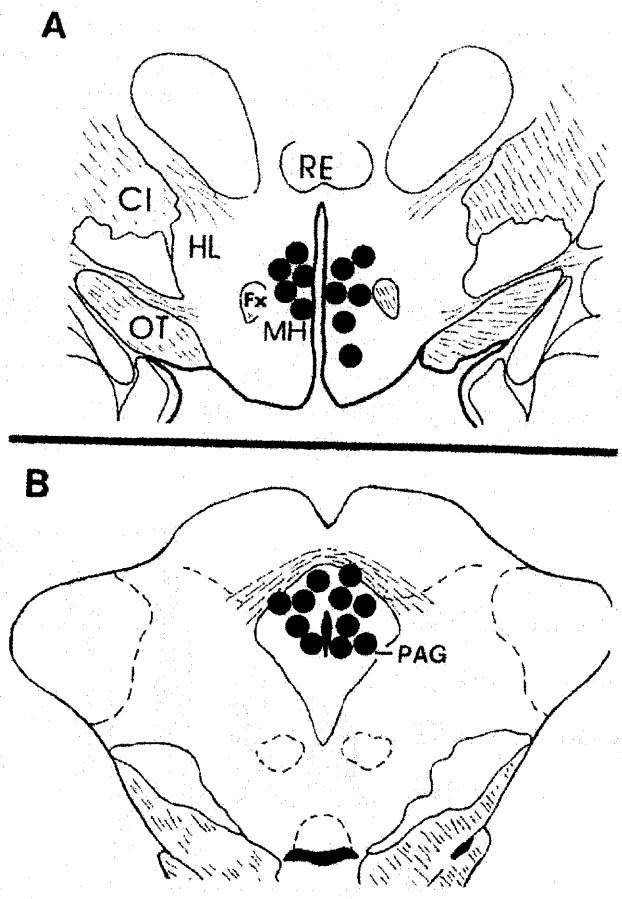

Fig. 2.1 Maps of Sites in: (A) Medial hypothalamus from which defensive rage was elicited, and (B) PAG from which defensive rage was also elicited. abbreviations: CI, internal capsule; Fx, fornix; HL, lateral hypothalamus; MH, medial hypothalamus; OT, optic tract; PAG, midbrain periaqueductal gray; and RE, nucleus reunions.

The hissing response was used as the primary measure of defensive rage behavior since hissing always occurred with each trial of stimulation as an integral component of the defensive rage response. Response latencies for hissing were recorded with a stopwatch and response thresholds were determined as well. The latency for each response was defined as the duration of time required for a cat to initiate hissing following the onset of electrical stimulation of the medial hypothalamus. The response

threshold was defined as the lowest current value at which responses could be elicited on 50% of the trials. Increases in threshold and/or latency were interpreted as a measure of response suppression, while decreases in threshold and/or latency were interpreted as a measure of response facilitation. Current was raised or lowered in 0.05 mA steps in an a-b-b-a manner (with 'a' above threshold and 'b' below). The a-b-b-a method is the steps by which the behavioral response sites in the hypothalamus were elicited with the cannula electrodes.

2.5 Experimental Protocol

Prior to drug administration, cats were given 4 trials separated by a 2-min rest period of stimulation of the medial hypothalamus in order to determine baseline response threshold and latency values for hissing. Then, Prozac was injected (IP) into the stomach in doses of 3.4 cc. After a 5-min waiting period, groups of 4 trials separated by a 2-min rest period of hypothalamic stimulation were then repeated over the post-injection blocks of time: 5 min, 15 min, 30 min and 50 min.

2.6 EMG Recording Phase

After the establishment of a stable threshold current for eliciting an emotional behavioral response, the skin overlying the ipsilateral masseter muscle was shaved and cleaned with alcohol, and bipolar surface electrodes, 0.5cm in diameter, were affixed to the skin using tensive conductive adhesive gel (Parker Laboratories Inc, Fairfield, NJ), one overlying the angle of the mandibule, with the second having a 15mm inter-electrode distance over the masseter muscle and oriented parallel to the course of the muscle fibers. A ground electrode was attached to the skull. The EMG signals were preamplified and recorded

using a Grass S88 amplifier that rectified and integrated the signal. The data was acquired using data acquisition software, (LabView v6.0, National Instruments, Inc, USA) along with a 16-channel A/D National instrument data acquisition card, NI PCI-6025E, connected to a Gateway 400 MHz computer. The EMG signal was recorded with a bandwidth of 10 to1000 Hz with an acquisition rate of 2000 Hz, and stored in a computer for analysis. During each experiment, the animal was gently restrained to prevent removal of the electrodes attached to its face.

2.7 Data Analysis

Two types of data analysis were employed: statistical analysis and wavelet analysis.

The mean frequency (MF) of the electromyogram is a useful index of acute muscular response. However, for the masseter muscles, the MPF value has not been extensively investigated at different levels of muscular contraction and was employed in the data analysis phase of this research. In this study, the EMG signals were resolved by wavelet analysis into their intensities in time and frequency space. The intensity (square of wavelet coefficients) represents the power within the EMG for any given time and frequency band. The mean frequency used in this study is comparable to the mean power frequency used to measure EMG contractions [20]. There are three applications which dominate the use of the surface EMG signal: its use as an indicator for the initiation of muscle activation, its relationship to the force produces by a muscle, and its use as an index of the fiber recruitment processes occurring within a muscle. The use of the EMG signal to provide an "emotional response index" has considerable appeal because it has been shown that the signal displays time-dependent changes prior to any force

modification, thus having the potential to predict the onset of contractile activity related to emotional behavior.

The wavelet transform and the mean power frequency (MF) were calculated for each interval. The mean frequency was chosen for this analysis because it is a more accurate representation of recruitment and rate coding in the muscle than the median frequency and is also less sensitive to variations in conduction velocity and noise or interference [18]. The idea was to relate the physiology of the muscle (i.e. the emotional response index) to the signal processing. It is important to note that the deterministic part of the signal may undergo abrupt changes such as a jump, or a sharp change, or very rapid evolutions such as transients in this dynamic system (EMG). The main characteristic of these phenomena is that the change is localized in time or in space. Therefore, the use of the wavelet analysis in this research was to determine the following parameter of the EMG signals between sessions.

Total shift of MF: MF (mean frequency) is the frequency value, separating the power spectrum into two equal surface regions. Using the wavelet power spectrum, which is, in full analogy to the power spectrum used in Fourier analysis, given by the square of the wavelet coefficients [21], it is expected to show that the emotional response of the muscle contraction i.e. late stimulation, had on average, fewer high frequency components than early stimulation and therefore the mean frequency will be lower. The Slope of MF (frequency response rate) with time would be used as a comparative index among subjects during the analysis of the data. It is expected to show the suppression of frequency response due the infusion of SSRI over time. The local aspects of the wavelet analysis are well adapted for processing this type of event, as the processing scales are

modification, thus having the potential to predict the onset of contractile activity related to emotional behavior.

The wavelet transform and the mean power frequency (MF) were calculated for each interval. The mean frequency was chosen for this analysis because it is a more accurate representation of recruitment and rate coding in the muscle than the median frequency and is also less sensitive to variations in conduction velocity and noise or interference [18]. The idea was to relate the physiology of the muscle (i.e. the emotional response index) to the signal processing. It is important to note that the deterministic part of the signal may undergo abrupt changes such as a jump, or a sharp change, or very rapid evolutions such as transients in this dynamic system (EMG). The main characteristic of these phenomena is that the change is localized in time or in space. Therefore, the use of the wavelet analysis in this research was to determine the following parameter of the EMG signals between sessions.

Total shift of MF: MF (mean frequency) is the frequency value, separating the power spectrum into two equal surface regions. Using the wavelet power spectrum, which is, in full analogy to the power spectrum used in Fourier analysis, given by the square of the wavelet coefficients [21], it is expected to show that the emotional response of the muscle contraction i.e. late stimulation, had on average, fewer high frequency components than early stimulation and therefore the mean frequency will be lower. The Slope of MF (frequency response rate) with time would be used as a comparative index among subjects during the analysis of the data. It is expected to show the suppression of frequency response due the infusion of SSRI over time. The local aspects of the wavelet analysis are well adapted for processing this type of event, as the processing scales are

connected to the speed of the change. The subsequent analysis was based on daubechies 6 "db6" which is well suited to analyzing EMG signals. The accuracy of the continuous wavelet transform C(t) was limited by the following factors: First, by the spectral resolution of the analyzing wavelet. Secondly, by the significance of the coefficients of the wavelet power spectrum which decreases towards the boundaries of the signal. Thirdly, by the background noise inherent in the EMG signal [41].

Statistical comparisons using ANOVA (two-factor without replication and single-factor without replication) was performed (significance level: 0.05). The null hypothesis (H_o) assumes the equality of the compared parameters (mean values of early and late stimulation among the three cats). If F-calculated is greater than the F-critical, reject the null hypothesis. If the P-value is less than the confidence interval of 0.05, reject the null hypothesis.

2.8 Time-Frequency Analysis using the Continuous Wavelet Transform (CWT)

The EMG signals in this study were sampled at a rate of 2000 Hz. They were run through a Labivew program that removed the DC component and the chance for a biasing effect by bandpassing the data from 3 to 750 Hz, as per the Nyquist sampling theorem. The majority of the power in the signals elicited from both behavioral states was centered at less than 200 Hz as shown in figure 4.1a. The data were also filtered from 18 to 22 Hz to remove stimulation artifacts and 57.5 to 63 Hz to remove 60 Hz noise from the electric lines. The filtered EMG files were then run through the Matlab wavelet program outlined in Appendix B to perform the continuous wavelet transform on the signal. This analysis

employs the Daubechies order 6 (DB6) wavelet. The rationale for choosing this particular wavelet, as well as a discussion of wavelet technique, is the topic of Chapter 3.

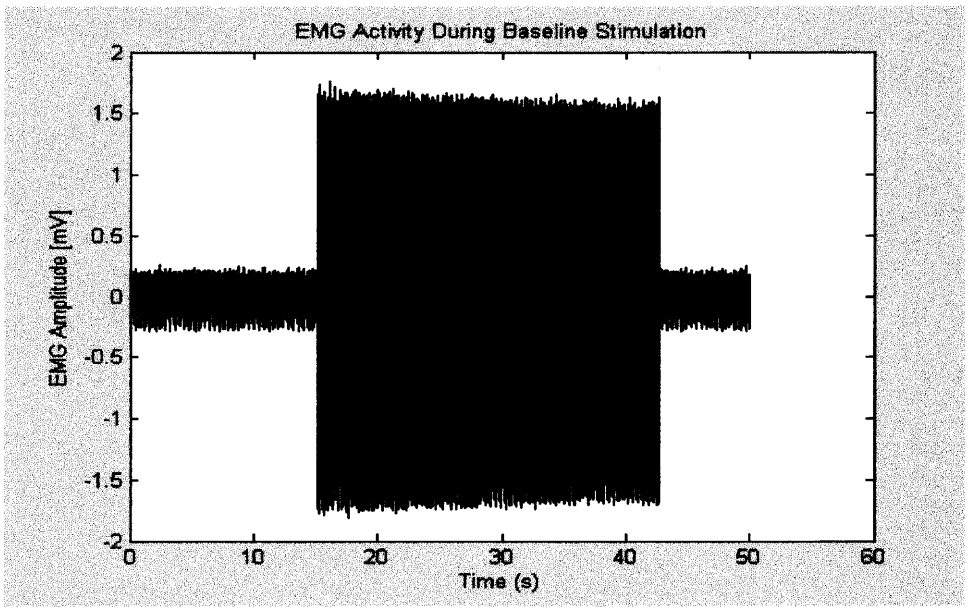

Figure 2.2 Time-Amplitude plot of EMG activity during baseline stimulation

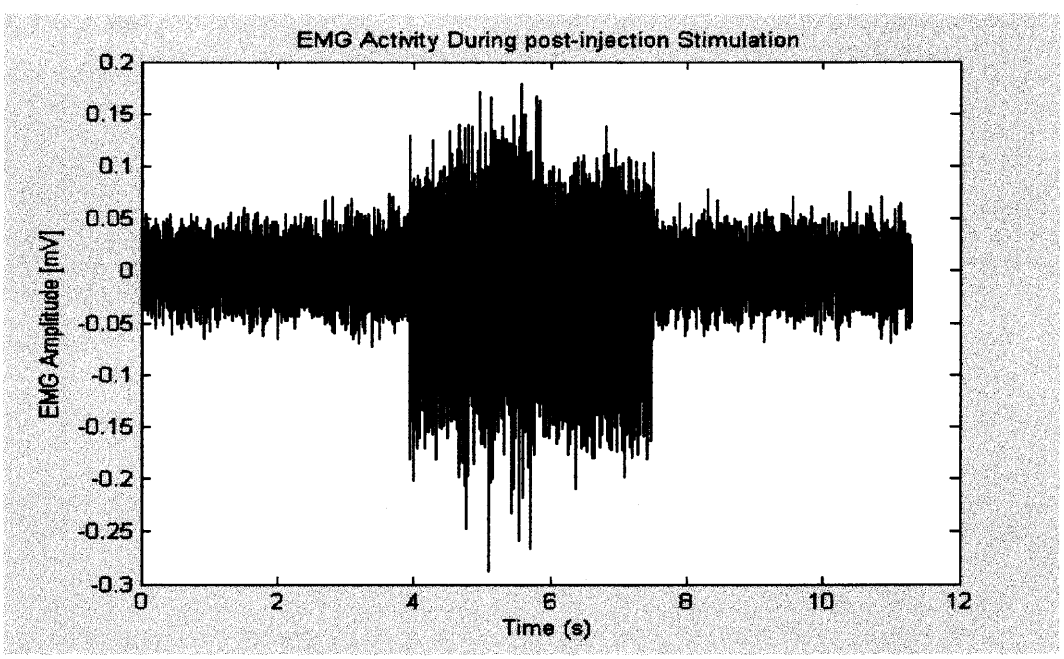

Figure 2.3 Time-Amplitude plot of EMG activity during post-injection stimulation

Figure 2.2 illustrates the time-amplitude representation of the EMG recorded during baseline hypothalamic electrical stimulation, while Figure 2.3 is the time-amplitude representation of the EMG signal recorded during post-injection stimulation. Note that in Figure 2.2, the stimulation begins with the first large jump in EMG amplitude and ends with the return to the pre-stimulation baseline level. In figure 2.3, the effect of the drug occurring in the locations where there are large variations of the amplitude of the signal. The post-injection signal displays spikes in activity, whereas the baseline signal displays no variation in amplitude throughout the length of the stimulation. The magnitudes of the two signals are approximately order of ten different from each other, signifying differences in EMG amplitude between the two stimulation states.

CHAPTER 3

THE MATHEMATICS OF WAVELET TIME-FREQUENCY ANALYSIS

Studies that have examined the role of the nervous system in the modulation of the recruitment of muscles have been limited to the evaluation of electromyographic signals in either the time or frequency domains [29, 30, 31]. These studies have yielded valuable information about the role of hypothalamically induced neuromuscular activity in comparison to cortically invoked activity. Results from these studies indicate that the values of EMG amplitude and mean power frequency obtained during hypothalamic stimulation were significantly higher than those observed during mastication. The studies have thus indicated that there is a correlation between hypothalamic stimulation and increased EMG activity in both time and frequency measures. It is thought that the shift in mean power frequency is indicative of a more extensive recruitment of rapidly fatiguing muscle fibers, as well as an increase in motor neuron firing frequency. However, previous studies have not been able to clearly define the role of the nervous system in the modulation of the recruitment of the fibers of the masseter muscle. This is because at the time the studies were performed, the computing capability and signal analysis techniques were limited. This resulted in the lack of either time or frequency resolution, depending upon the type of analysis performed.

The hypothalamus is thought to activate the stress response and thereby modulate the level of activity in the masseter muscle, which is controlled mainly by the cortex and basal ganglia during voluntary muscular activity. The past studies have been limited in the respect that the data analyses in the time domain are missing critical information

regarding the frequency content of the signal, whereas the frequency analyses are missing time resolution. The studies were able to identify that in the time domain the amplitude of the EMG signal changed at specific times during the experiment. They also identified that the average power of the frequency was different between the two behavioral states. This indicates that the muscle activity varies between the two behavioral states, but is not enough information to clearly define what is causing the changes in EMG amplitude at specific times. It is also not enough information to clearly define what is causing the changes in mean power frequency. The averaged power only accounts for specific frequency content that is averaged over the length of the signal. This gives an indication of which frequencies are the most active in the signal, but it does not give time information that would indicate what frequencies are active at which times. A combination of time and frequency information would elucidate the ways in which the muscle recruitment is modified by the stress response.

A method of combining the two attributes of time and frequency without losing critical time or Fourier parameter information is through the implementation of time-frequency decomposition. This method of evaluating non-stationary signals that contain transient components has been gaining increasing popularity, with the first implications for applications to signal analysis in the 1940s. Recently, a time-frequency method has come to the forefront as a powerful method of analyzing transients and allowing the researcher to investigate frequency components over the length of the signal. This method, known as the Wavelet Time-Frequency Multi-Resolution analysis, makes it possible to have good time and frequency resolution due to a shape that is other than a sinusoid and is applied to the signal using a scalable window.

A shortcoming of time-frequency decompositions based upon the Fourier transform is the inability to use a scalable window, which results in the loss of time resolution. The Fourier transform based methods of time frequency analysis are based upon scaling and shifting a sinusoid and convolving it with signal to be analyzed, using a fixed window of time for all frequencies. Another shortcoming of this method is that because sinusoids are infinite signals in time, they are not contained completely in the window that is chosen for the analysis. For this reason, the use of a sinusoid introduces artifact into the analysis due to the fact that the window captures different quantities of periods of the sinusoid at different frequencies, depending on window size being used.

The wavelet transform uses the theory of time-frequency decomposition and employs an adaptive window size that changes based upon the frequency being examined. It also employs basis signals other than sinusoids in the analysis. The basis signals for this type of analysis are called wavelets. The signals employed in the wavelet analysis decay to zero exponentially, reducing the problem of the base extending outside of the window and the associated introduction of artifact. They also oscillate about zero in the time domain and therefore possess a zero mean value. Translated to the frequency domain, the Fourier transform of the wavelet must approach zero at the zero frequency, which forces a band-pass behavior of the wavelet. This time and frequency characteristic of the wavelet is referred to as the *admissibility condition*, which must be met in order for reconstruction of the signal using wavelet coefficients [32]. The requirements for wavelet construction and implementation are discussed in detail in Section 3.2.2.

The Fourier transform utilizes the infinitely bound sine wave as the basis for analysis. This enhances the likelihood of missing small transients in signals that the

wavelet would detect due to its limited duration. The wavelet, then, is well suited to analyze a local area of a signal that would otherwise be missed by the traditional Fourier analysis. The shape of the wavelet is typically asymmetrical as compared to the Fourier transform, which utilizes the uniformly shaped sinusoid. The shape of the wavelet renders it well suited to detection in signals that contain sharp changes in frequency content.

Another quality of the Daubechies family of wavelets that makes them useful techniques in non-stationary signal analysis is that they are orthogonal. This attribute causes the wavelet coefficients to be orthogonal. In turn, this causes each wavelet coefficient to be representative of independent signal components [33]. For example certain wavelets, such as the Morlet, Gaussian and Mexican Hat, are not orthogonal.

The wavelet method is unlike other time-frequency decomposition methods because it is not based upon the traditional Fourier base of sinusoids and does not use fixed windows of time to analyze the signal at all frequencies. The window size varies depending upon the scale, or frequency, that is being investigated. In addition, the wavelet method convolves a "mother wavelet," of shape and duration varied by the class of wavelet and the scale being assessed, with the signal to be analyzed. This mother wavelet is scaled and shifted based upon the frequency band of interest. This scaling and shifting allows for the detection of small transients as well as larger trends within the data. It also allows for better time and frequency resolution that traditional methods have provided. A wavelet analysis is the method chosen for this work. The construction and implementation of the Continuous Wavelet Transform will be discussed in this chapter.

3.1 History of the Wavelet Transform

The wavelet time frequency decomposition is a mathematical theory that has been in development since the early 1900s. Alfred Haar, in 1909, is credited with the first written description of the theory that has since become referred to as wavelet analysis. Since then, the theory has gained increasing popularity. In 1988, Stephane Mallat derived the algorithm that is the basis for this approach to time-frequency analysis [34]. Since then, engineers have embraced this method in various fields of research, including but not limited to acoustic emission [35, 36], transmission line fault detection and protection [37] and detection and classification of material attributes [38]. Recently, biomedical applications of the wavelet analysis, such as the analysis of motor unit action potentials [39] and the use of electromyography for the detection of back muscle fatigue [11], began to appear in the literature.

The theory of wavelet based decomposition of signals is founded upon the nineteenth century theory presented by Joseph Fourier, which has come to be known as the Fourier analysis or Fourier transform, whereby a signal is decomposed into its frequency components via the use of sinusoids. The wavelet transform replaces the time information lost in the Fourier transform. Wavelet analysis performs a frequency analysis that assesses frequency band activity over time, rather than calculating the sum of all frequency activity during the life of the signal of interest. Today, United States mathematicians, such as Daubechies and Coiflet, lead the research that is aimed toward the advancement of wavelet theory [34].

3.2 Implementation of the Wavelet Transform

The Continuous Wavelet Transform (CWT) uses a main signal, referred to as the "mother wavelet" and convolves a shifted and scaled version of this signal with the signal to be analyzed. Mathematically, this approach is represented by the equation

$$C(a,p) = \int_{-\infty}^{\infty} f(t)\psi^*(a,p,t)dt \tag{3.1}$$

where C represents the coefficients that are a result of the product of the original function and the conjugate of the mother wavelet, a represents the scaling factor of the mother wavelet, p is the shifting factor of the mother wavelet, $f(t)$ is the original signal and $\psi^*(a,p,t)$ is the conjugate time-dependant mother wavelet, scaled and shifted by a and p, respectively. The mother wavelet is decomposed via scaling and translation into a set of smaller basis functions, represented by ψ_{ap}, where

$$\psi_{ap}(t) = \frac{1}{\sqrt{a}}\psi\left(\frac{t-p}{a}\right), \tag{3.2}$$

and $a^{-1/2}$ provides energy normalization across scales.

Scaling is the process by which the wavelet is stretched or compressed at a certain level, as seen in Figure 3.1. This scaling or compressing enables the wavelet to capture frequency information at various frequency levels. Higher frequency content is captured at lower scales and conversely, lower frequency content is captured with higher scales.

Scales are in powers of 2. For example, a scale factor of 9 corresponds to a level of 2^9, or 512, wavelet coefficients. At higher scale levels the wavelet analysis possesses greater

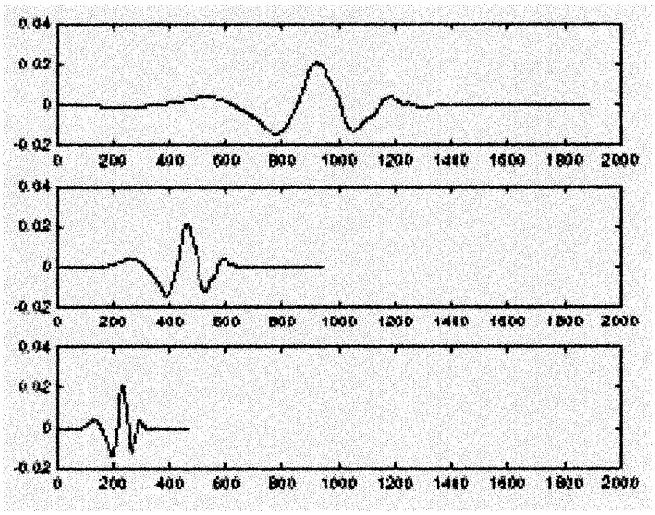

Figure 3.1 Scaling the mother wavelet. Note that the signal becomes increasingly short in duration at smaller scales. This yields information about quickly changing, or the high frequency content of, signals.

frequency resolution, whereas lower scale levels yield better time resolution because decreasing the scale parameter increases the width of the wavelets, as shown in Figure 3.2 [40]. The bandwidth decreases by half at every scale. This enables higher frequency resolution at higher scales, or lower frequencies. Conversely, it enables higher time resolution at lower scales, or higher frequencies. Wavelet representations are typically referred to as time-scale decompositions due to the fact that the mother wavelet is compared to the original signal in scales, not frequency.

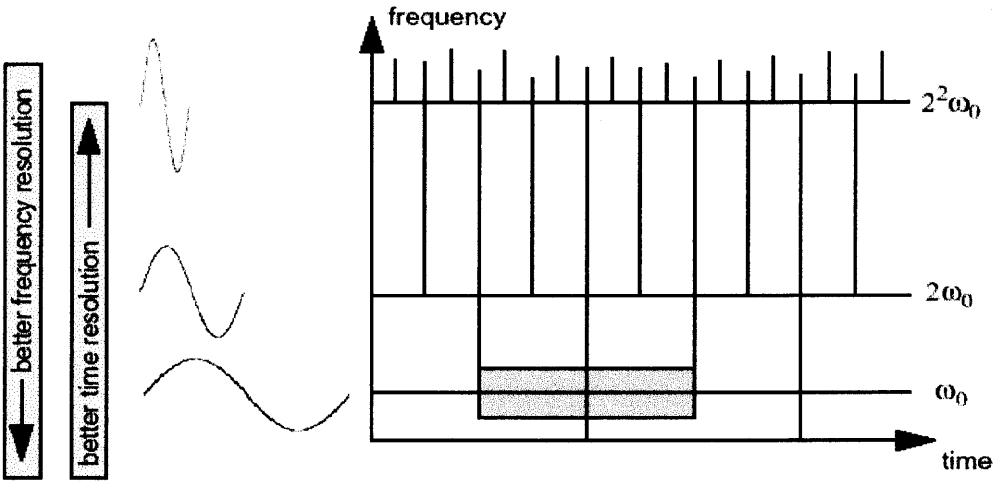

Figure 3.2 Wavelet transform scaling grid. Scale is approximately equivalent to the inverse of frequency. Note that scale increases in the opposite direction of the frequency. As frequency increases, scale decreases. As the scale decreases, the duration of the wavelet decreases, enhancing the time resolution of the wavelet at higher frequencies.

However, frequency roughly correlates to the inverse of the scale value and is related to the scale in the following way:

$$F_a = \frac{F_c}{F_s a}, \tag{3.3}$$

where F_a is the frequency correlating to a specific scale, F_s is the sampling frequency, F_c is the center frequency of the specific mother wavelet at the scale being analyzed and a is the scale being analyzed. The scaled wavelet is then shifted across all time of the signal.

Shifting is the process by which the onset of the application of the mother wavelet

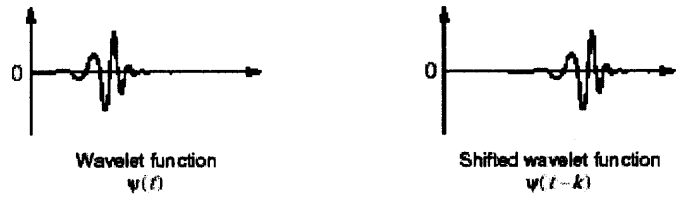

Figure 3.3 Shifting the mother wavelet. In this case, ***k*** is the shifting factor, or the length of time by which to delay the onset of the application of the wavelet.

is delayed or hastened, as can be seen in Figure 3.3 [34]. This allows for the time component in the wavelet analysis. Rather than looking at specific windows of time, the wavelet analysis looks at all time in the duration of the signal being analyzed, at varying scales. Higher scales will yield larger shifts in time in order to capture the activity at lower frequencies. Likewise, lower scales yield smaller shifts in time, in order to capture the activity at higher frequency, or rapidly changing, content of the signal.

Wavelets address problems with inaccuracies of representation of the frequency content of a signal as a result of Fourier analysis based time-frequency analyses. It does this by convolving the signal to be analyzed with a signal that meets two specific properties: the *admissibility* and the *regularity* conditions. The admissibility condition requires that the wavelet decay quickly to zero outside of the time and frequency of interest. This property of wavelets is known as the *localization property* of the wavelet. In the time domain, this is equivalent to saying that the wavelet must oscillate about zero and have a mean value of zero. In the frequency domain, this is equivalent to the statement that the wavelet is *compactly supported,* or *band limited*, and must decay quickly to zero outside of the frequency band of interest. This concept is represented mathematically in Equations 3.4 and 3.5.

$$\int \psi(t)dt = 0 \tag{3.4}$$

$$|\psi(\omega)|^2_{\omega=0} = 0 \tag{3.5}$$

That is, the mother wavelet signal exists only in the local region of the signal. These two combined attributes of the wavelet transform are collectively referred to as the *admissibility condition*, which is part of the requirement that must be met for the signal to be considered a wavelet.

The fact that wavelets decay in both the time and frequency domains results in an analysis that possesses very good time and frequency localization. However, it is impossible to have perfect accuracy of analysis due to Heisenberg's uncertainty principle. In the application of this theory to signal analysis, the principle states that it is impossible to obtain information about an exact frequency and exact time at which that frequency occurs. That is, it is impossible to get exact information about both time and frequency for any given time or frequency [41].

The regularity condition, which is the other portion of the requirement for a signal to be considered a wavelet, states that wavelet transforms must decay quickly with decreasing scale and employs the concept of vanishing moments. The concept of vanishing moments can best be described as the points at which the derivatives of the function are equal to zero. Equation 3.6 defines the moment, M_p, of the wavelet as

$$M_p = \int f^p \psi(t)dt \,, \tag{3.6}$$

where f^p is the pth derivative of f and $\psi(t)$ is the wavelet. Recall from Equation 3.4 that M_p equals zero, based upon the above equation. Expanding Equation 3.1 to the nth term using a Taylor expansion yields

$$C(a,0)=\frac{1}{\sqrt{a}}\left[f(0)M_0a+\frac{f^{(1)}(0)}{1!}M_1a^2+\frac{f^{(2)}(0)}{2!}M_2a^3+\ldots+\frac{f^{(n)}(0)}{n!}M_na^{n+1}+X(a^{n+2})\right], \tag{3.7}$$

where the translation, or shifting, coefficient p is set to zero for simplicity and X is the remainder of the expansion [42]. Implementing Equations 3.4 and 3.6, the terms with moments approach zero and the value of the wavelet transform coefficients decay as fast as a^{n+2}. The higher n is, the faster the signal decays. This is what is meant in wavelet analysis by the *regularity condition.* That is, as the number of vanishing moments increases, the shape of the wavelet becomes smoother, or more *regular.* The number of vanishing moments is equivalent to n. For the Daubechies family of wavelets, n is theoretically infinite, rendering the wavelet ideal for many diverse applications.

In summary, the wavelet should meet the conditions of admissibility and regularity. The admissibility condition allows the wavelet to be used in applications where perfect reconstruction of the original signal is necessary. It also ensures that the regularity condition may be met by forcing the moments to zero.

3.3 Use of the Daubechies Order 6 (db6) Wavelet

The wavelet analysis was performed using Matlab version 6.1, with the Wavelet toolbox. The program is included in Appendix B. The data files were filtered as discussed in 2.4.4

using a Labview version 5.1 program, which is included in Appendix A. The EMG data are fast varying signals with transients of short duration.

Lower order Daubechies wavelets are well suited to provide high time resolution in the higher frequency scales [43]. This enables the lower order Daubechies wavelets to capture short transients, which is important when assessing bursts of neuromuscular activity. The transition from levels of higher EMG activity to lower activity may yield important information about motor neuron activation timing, targeting and power. Transient frequency components may also yield insight into the recruitment patterns of the masseter muscle during different behavioral states.

The Daubechies family of wavelets can also be used in continuous or discrete transformations. This is an important aspect to consider, depending upon the desired application. A part of this study assessed whether wavelets could provide an accurate reconstruction of the original signal once decomposed. The Discrete Wavelet Transform (DWT) is necessary for the reconstruction of the wavelet. This is true because the discrete wavelet transform down-samples the signal by a factor of two per scale during the signal decomposition. Down sampling is necessary because in the wavelet analysis, both the details (high frequency component of the signal at a given scale) and approximations (low frequency content of the signal at a given scale) create a signal that is the same length as the original signal. The difference in numbers of coefficients between the discrete and continuous analyses is illustrated in Figures 3.4a and b. The images illustrate the filtering of the original signal, $\boldsymbol{S}$. The signal is low passed to create the approximations set of coefficients. $\boldsymbol{S}$ is also high passed to create the details set of coefficients.

In Figure 3.4a, the continuous wavelet transform (CWT), the details and approximations values are not down-sampled. This results in approximation and detail signals that are each the length of the original signal. If the two sets of coefficients from the CWT are combined, the resultant signal contains twice the amount of data as is contained in the original signal.

In contrast, in the discrete wavelet transform (DWT), illustrated in Figure 3.4b, the details and approximations are downsampled by two. The discrete wavelet decomposition removes every other point from the details and approximations, yielding decomposition values that are each half the length of the original signal. Yet, the signal integrity is not lost. Reconstruction of the signal using the discrete coefficient set yields a signal that is equal in length to the original signal.

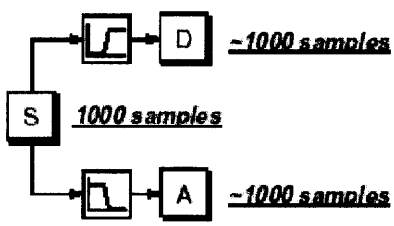

Figure 3.4a Filtering techniques involved with the continuous wavelet transform (CWT).

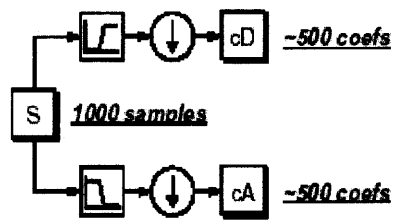

Figure 3.4b Filtering techniques involved with the discrete wavelet transform (DWT).

During reconstruction of the signal, the algorithm needs to upsample the details and approximations signals by a factor of two, as illustrated in Figure 3.5, which can only be done if the original decomposition was done discretely. Upsampling involves placing a zero between discrete points in the details and approximations signals, as shown in Figure 3.6. The resulting reconstructed signal is equal in length to the original signal.

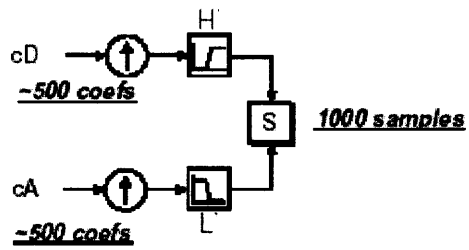

Figure 3.5 Reconstructing the original signal using the DWT coefficients.

The CWT does not provide a signal that can have a zero inserted at every other point and not lose the signal integrity. The CWT yields a smoother frequency analysis and ultimately yields a more complete picture of the frequency activity in the original signal and was thus chosen for the analysis aspect of this research.

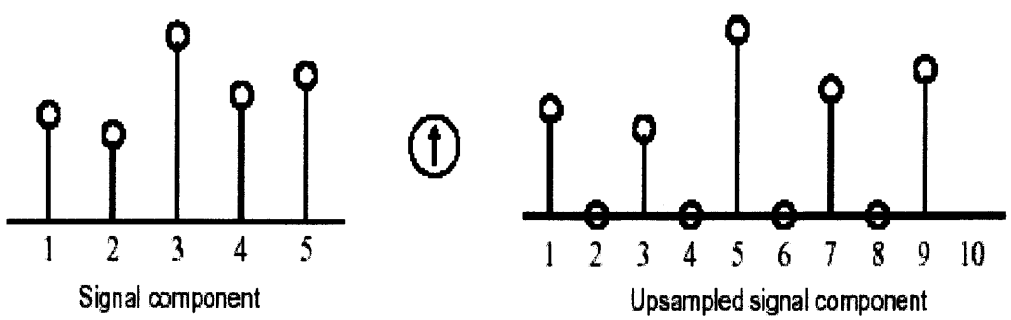

Figure 3.6 Zero insertion between coefficients. The arrow pointing upwards indicates that the upsampling has taken place. Note that the same arrow is present in Figure 3.5, which displays the filtering that takes place during reconstruction.

Figure 3.7 Daubechies Order 6 (db6) wavelet.

A lower middle level Daubechies wavelet, the db6 wavelet, was chosen for this research to ensure the accurate capture of transients and to provide high time resolution of those signal components. The wavelet is defined in terms of six coefficients, and the graph of it is shown in Figure 3.7. In summary, the features of the Daubechies wavelet that made it applicable to this study include compact support, infinite number of vanishing moments, ability to perform both discrete and continuous transformations and high time-resolution at various frequencies.

the power of the signal after drug injection varies across all frequency ranges. Note that the plotting scale of the signals ranges from 0 to 4, but the power of the coefficients is higher in the post injection signal than in the baseline signals. It is also noteworthy to see that the stimulation latency times are short in the post-injection signals than in the baseline signals.

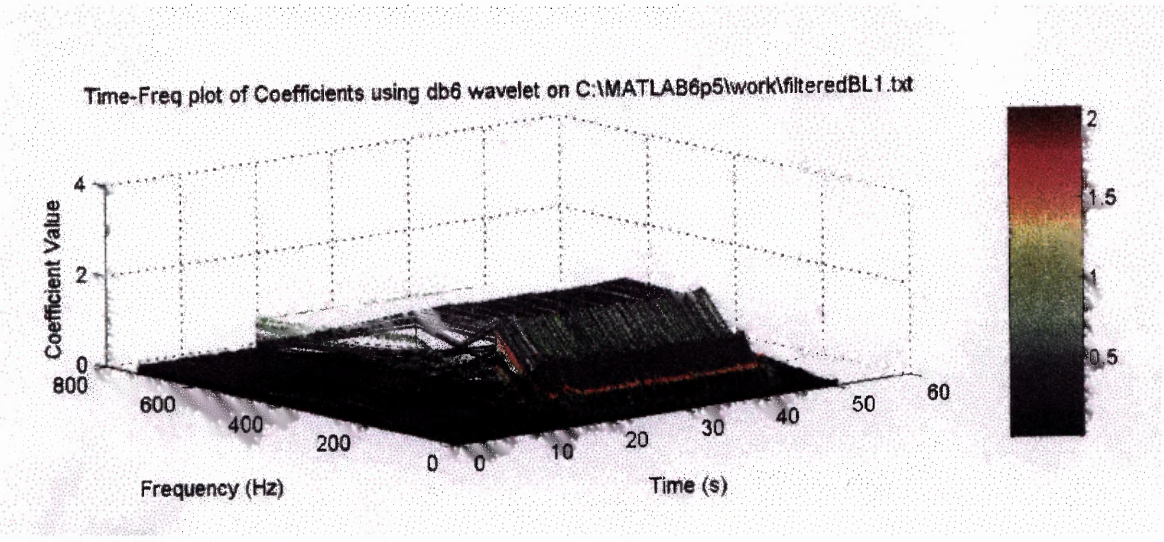

Figure 4.1a 3-D plot of the Continuous wavelet transform pre-injection (Baseline) stimulation. The frequency activity in the 3-30 Hz range does not possess power comparable to that seen in the 300-400 Hz frequency range

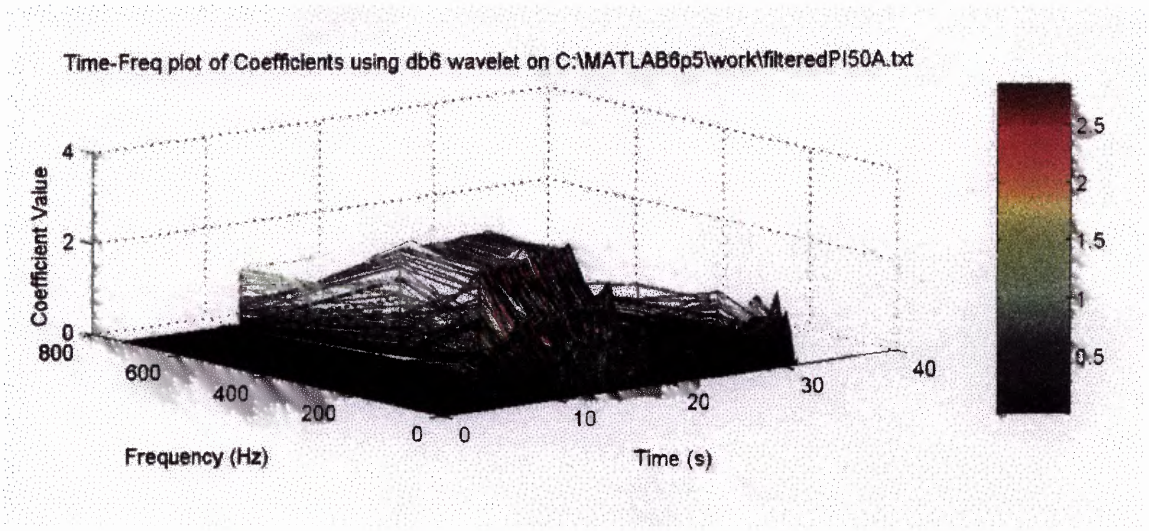

Figure 4.1b 3-D plot of the Continuous wavelet transform 50 minutes Post-Injection Note the downward shift in frequency activity from 300-500 Hz to the 75-200 Hz range. The high power activity is located in the 3-30 Hz range

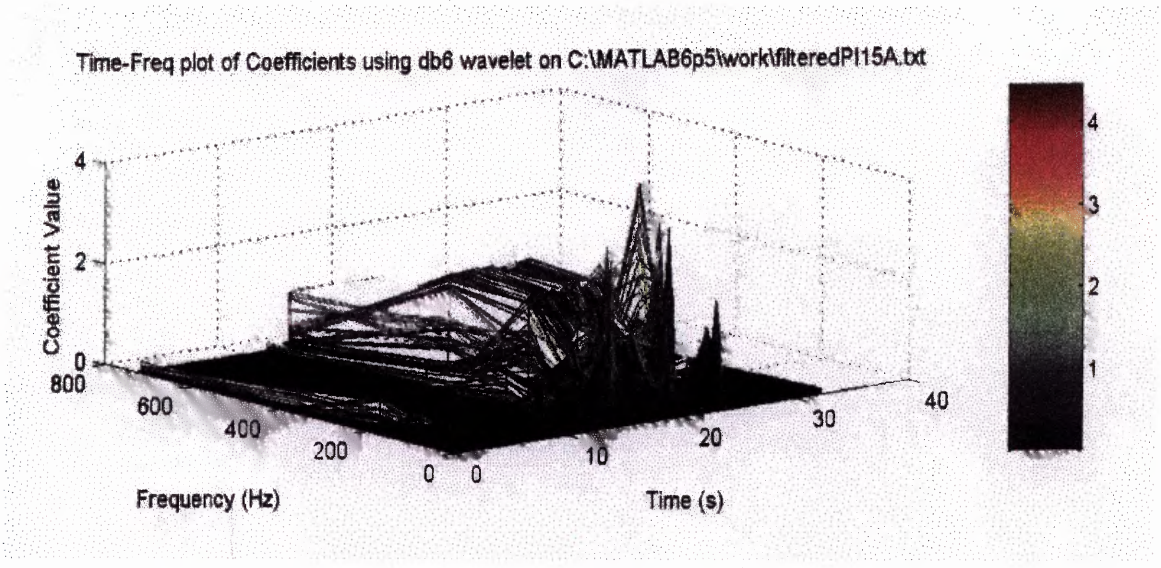

Figure 4.2 3-D plot of the Continuous wavelet transform 15 minutes Post Injection

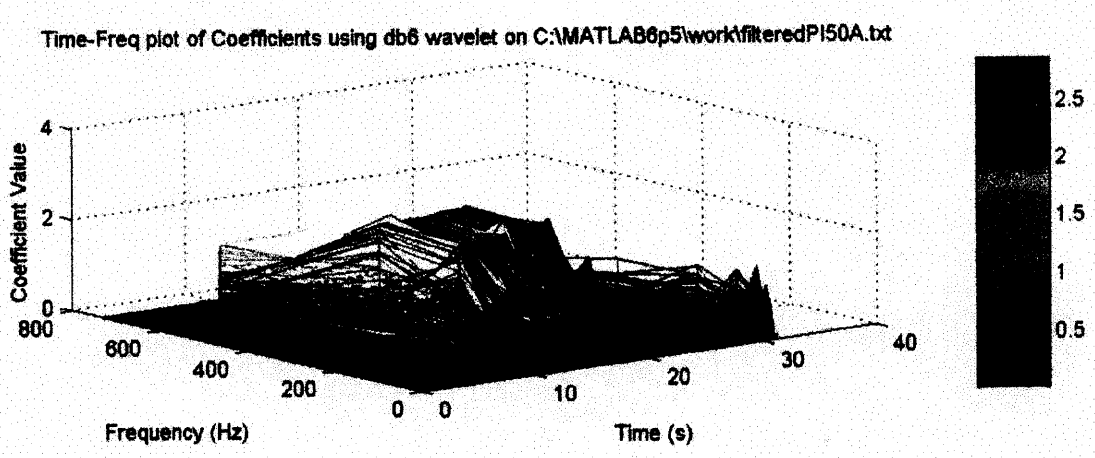

Figure 4.1b 3-D plot of the Continuous wavelet transform 50 minutes Post-Injection Note the downward shift in frequency activity from 300-500 Hz to the 75-200 Hz range. The high power activity is located in the 3-30 Hz range

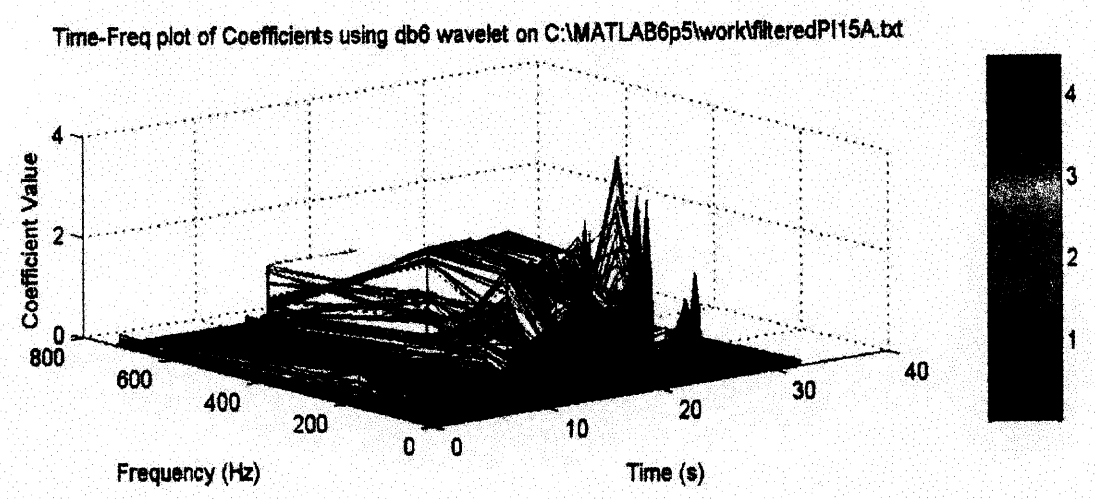

Figure 4.2 3-D plot of the Continuous wavelet transform 15 minutes Post Injection

4.2 Calculation of the Mean Frequency parameter

The mean frequencies (MF) were estimated from the power spectrum. Surface electromyogram (SEMG) MF has been proved to be a reliable descriptor of the muscle fatigue evolution in the isometric exercise. MF was chosen as the preferred parameter to median frequency (MDF) due to its smaller standard deviation [18]. Statistically, it is shown theoretically that MF is an unbiased estimator and that the MDF is convergent in the probability sense. The MF trends of EMG signals were analyzed further. From the MF trend of the EMG signal, an average of the 5-second blocks of the signal were calculated and concatenated after each iteration, to maintain the integrity of the frequency resolution. This was done due to the limitations in handling large samples of data and large memory requirements in Matlab. The results can be seen in figure 4.3a thru 4.4c.

In order to have a better visual representation of the shift in mean frequency and to statistically quantify the data between early and late stimulation, the continuous wavelet transform was employed. Figure 4.3a – 4.3c shows early stimulation average mean frequency plot Vs time in each subject, while Figure 4.4a – 4.4c shows late stimulation average mean frequency plot Vs time in each subject. It is noteworthy to point out that on average, the mean frequencies of the early stimulation are higher than the mean frequencies of the late stimulation as shown in table 4.1a and 4.1b. This can be seen as a downward shift from higher frequencies to lower frequencies, which is indicative of fatigue episode.

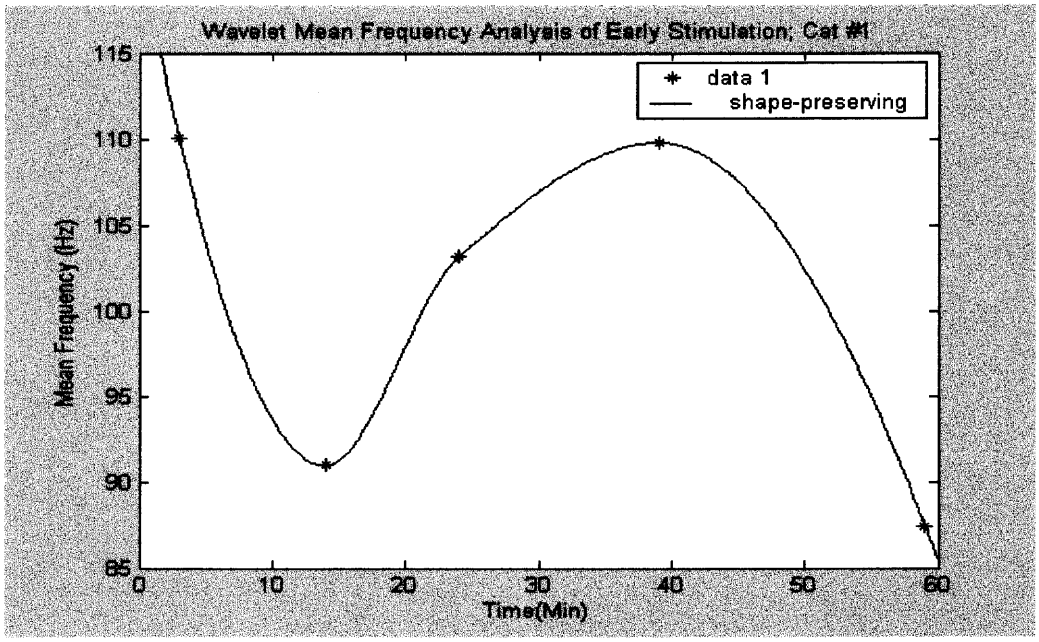

Figure 4.3a Plot of Average mean frequency of each trial block during early stimulation in cat #1

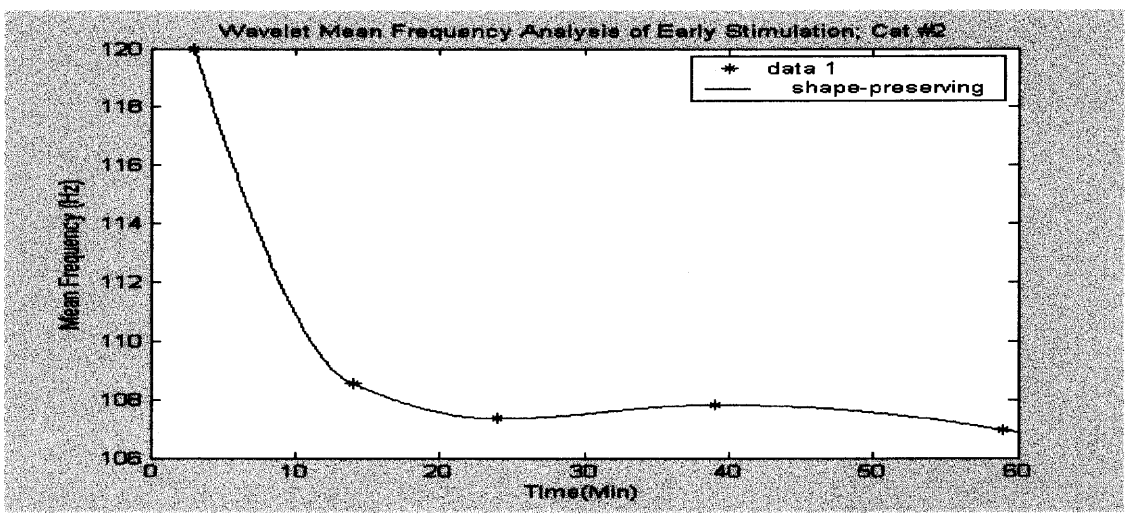

Figure 4.3b Plot of Average mean frequency of each trial block during early stimulation in cat #2

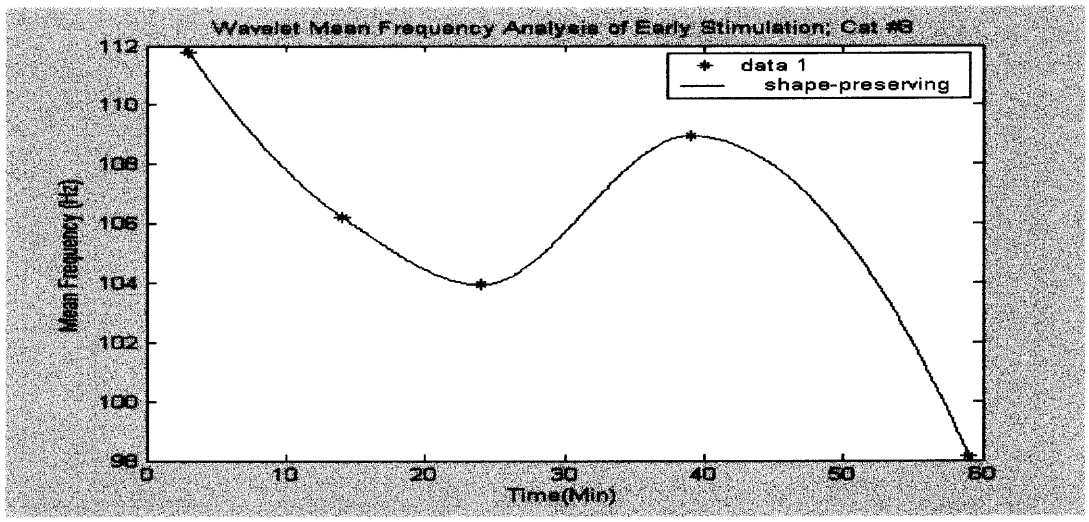

Fig. 4.3c Plot of Average mean frequency of each trial block during early stimulation in cat #3

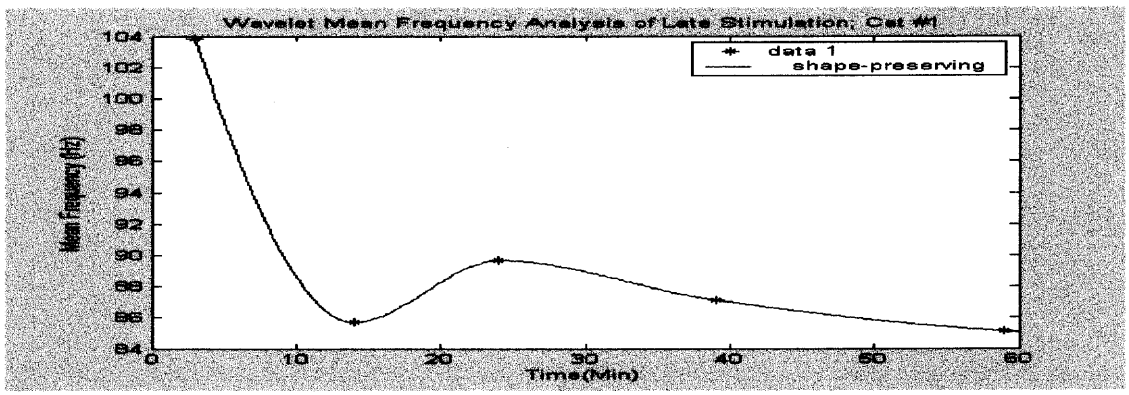

Figure 4.4a Plot of Average mean frequency of each trial block during Late stimulation in cat #1

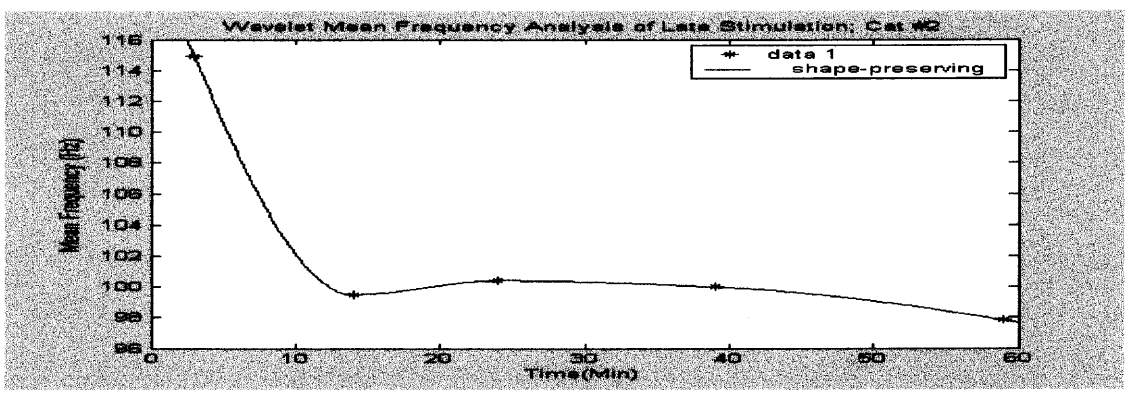

Figure 4.4b Plot of Average mean frequency of each trial block during Late stimulation in cat #2

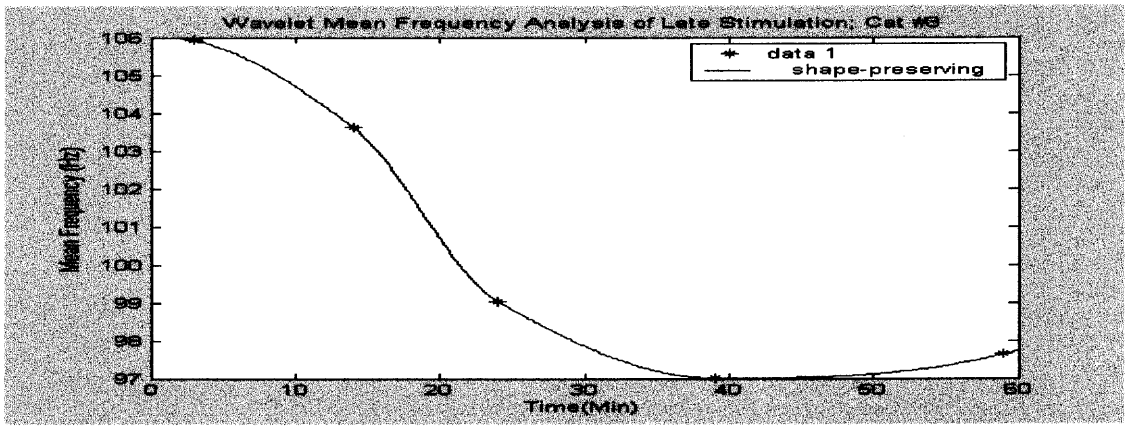

Figure 4.4c Plot of Average mean frequency of each trial block during Late stimulation in cat #3

4.3 Statistical Analysis

Table 4.1a and 4.1b detail the mean frequency values of the individual subject data at different stimulation states and their averages within each trial block during early and late stimulation behavioral states. The early stimulation state was chosen to be between the time the electric switch was pressed and 5 sec after that (10,000 data points, Fs 2000 Hz per sec). The choices of the time block were chosen with respect to the constraints imposed by variation of the stimulation response time. The late stimulation state was chosen to be between the time the stimulation response was elicited and 5 sec before elicitation. The data selection intervals were also chosen with respect to the constraints imposed by the variations in response latency.

The letters A, B, C, and D as shown in table 4.1a and 4.1b are the different stimulation states within each trial block. A trial block represents a pre-defined time period in which four different stimulation trials; separated by a two minute waiting period

were conducted. There were five different trial blocks namely: Baseline, 5min post-injection, 15min post-injection 30min post-injection, and 50min post-injection as shown in table 4.1a and 4.1b. The time period between trial blocks was determined to be the summation of the waiting period between stimulation states and time period leading up to the next trial block.

Early Stimulation Mean Frequencies

Trials	*Cat #1*	*Cat #2*	*Cat #3*
Baseline A	103.59	114.54	127.81
Baseline B	105.91	126.99	100.04
Baseline C	115.15	120.07	110.62
Baseline D	115.46	118.34	108.65
Average Frequency	110.0275	119.985	111.78
Post injection 5min A	99.39	108.46	109.48
Post injection 5min B	91.43	112.15	100.73
Post injection 5min C	86.04	109.9	108.56
Post injection 5min D	87.02	103.69	106.14
Average Frequency	90.97	108.55	106.2275
Post Injection 15min A	90.7	125.05	106.66
Post Injection 15min B	117.79	100.87	108.11
Post Injection 15min C	110.78	97.77	102.15
Post Injection 15min D	93.59	105.72	98.85
Average Frequency	103.215	107.3525	103.9425
Post Injection 30min A	108.76	110.84	100.37
Post Injection 30min B	105.15	105.44	110.88
Post Injection 30min C	108.42	118.54	116.95
Post Injection 30min D	116.79	96.48	107.61
Average Frequency	109.78	107.825	108.9525
Post Injection 50min A	85.06	110.51	115.91
Post Injection 50min B	97.52	106.15	91.94
Post Injection 50min C	85.1	115.24	104.17
Post Injection 50min D	82.14	95.95	80.63
Average Frequency	87.455	106.9625	98.1625

Table 4.1a Mean Frequencies of the Three Cats on Different Trial Intervals During Early Stimulation.

Late Stimulation
Mean Frequencies

Trials	*Cat #1*	*Cat #2*	*Cat #3*
Baseline A	116.04	121.41	106.32
Baseline B	88.45	105.82	117.32
Baseline C	107.27	114.06	88.59
Baseline D	103.61	118.3	111.49
Average Frequency	103.8425	114.8975	105.93
5min Post injection A	75.16	94.32	114.52
5min Post injection B	84.7	87.72	113.12
5min Post injection C	98.62	101.21	86.35
5min Post injection D	84.38	114.76	100.5
Average Frequency	85.715	99.5025	103.6225
15min Post Injection A	95.1	89.35	108.11
15min Post Injection B	88.05	96.14	86.78
15min Post Injection C	78.09	92.74	88.87
15min Post Injection D	97.5	123.34	112.42
Average Frequency	89.685	100.3925	99.045
30min Post Injection A	90.44	97.93	99.54
30min Post Injection B	80.43	93.92	96.99
30min Post Injection C	87.54	109.45	98.85
30min Post Injection D	90.1	98.66	92.67
Average Frequency	87.1275	99.99	97.0125
50min Post Injection A	90.39	99.44	113.71
50min Post Injection B	80.98	87.72	85.46
50min Post Injection C	85.53	113.55	98.44
50min Post Injection D	83.6	90.59	92.97
Average Frequency	85.125	97.825	97.645

Table 4.1b Mean Frequencies of the Three Cats on Different Trial Intervals During Late Stimulation.

Average of Early Stimulation Frequencies

	Cat #1	*Cat #2*	*Cat #3*
Average of all Baseline Freq	110.0275	119.985	111.78
Average of all 5min Post injection Freq	90.97	108.55	106.2275
Average of all 15min Post Injection Freq	103.215	107.3525	103.9425
Average of all 30min Post Injection Freq	109.78	107.825	108.9525
Average of all 50min Post Injection Freq	87.455	106.9625	98.1625
Overall Average Frequency	100.2895	110.135	105.813

Table 4.2a Overall Mean Frequencies during Early Stimulation

Average of late Stimulation Frequencies

	Cat #1	*Cat #2*	*Cat #3*
Average of all Baseline Freq	103.8425	114.8975	105.93
Average of all 5min Post injection Freq	85.715	99.5025	103.6225
Average of all 15min Post Injection Freq	89.685	100.3925	99.045
Average of all 30min Post Injection Freq	87.1275	99.99	97.0125
Average of all 50min Post Injection Freq	85.125	97.825	97.645
Overall Average Frequency	90.299	102.5215	100.651

Table 4.2b Overall Mean Frequencies during Late Stimulation

Figure 4.2a and 4.2b detail overall mean frequency values during early and late behavioral states. The effect of drug upon latencies and response thresholds for defensive rage behavior over baseline and post-injection time periods were analyzed by Two-factor ANOVA without replication to test the over all effect of the treatments (early and late stimulation) on the experiment (effect of drug on the three cats). This was chosen to remove the effect of a nuisance factor (as a result of variations in the behavior of the individual cat such as hissing, unsheathing of the claws, and retraction of the ears). The null hypothesis assumes equal mean frequencies for the three cats on both activities (early and late simulation). The level of significance was set at $p = 0.05$. If $P < 0.05$, reject the null hypothesis and conclude that activities affect the sample statistic (mean frequency), which means that there is less than a 5% chance that the test would reject the null hypothesis if it was true. Table 4.3 shows the result of ANOVA for effect of activities on the overall average mean frequency values for the three cats.

There are significant differences between values obtained during early stimulation and late stimulation ($p = 0.03$) as shown in Table 4.3. $P < 0.05$ suggest that the mean

values for the two different states (early and late stimulation responses) are significantly different, and the differences cannot be attributed to a sampling error.

Anova: Two-Factor						
SUMMARY	***Count***	***Sum***	***Average***	***Variance***		
ACTIVITY						
Early Stimulation	3	316.2375	105.4125	24.35377		
Late Stimulation	3	293.4715	97.82383	43.34203		
SUBJECTS						
CAT 1	2	190.5885	95.29425	49.90505		
CAT 2	2	212.6565	106.3283	28.98269		
CAT 3	2	206.464	103.232	13.32312		
Source of Variation	***SS***	***df***	***MS***	***F***	***P-value***	***F crit***
ACTIVITY	86.38179	1	86.38179	29.6383	0.032123	18.51276
SUBJECTS	129.5625	2	64.78127	22.22698	0.043053	19.00003
Error	5.829066	2	2.914533			
Total	221.7734	5				

Table 4.3 Analysis of the Effect of Activity on the Overall Average Mean Frequencies.

Mixed results were obtained during the analysis of different trial blocks between early and late stimulation. While there was a highly significant difference when comparing baseline mean values among the three subjects during early and late stimulation ($p = 0.003$), There were no significant differences between the other stimulation blocks among the three subjects. Though there are differences among the mean values, statistically, the null hypothesis cannot be rejected given a 0.05 level of significance. While it is not conclusive, this difference could be attributed to effect of the drug on the subjects since the baseline simulation block is highly significantly different than the post-injection simulation blocks. However, this animal model illustrates that during emotionally mediated EMG activity, the magnitude of the EMG response is significantly higher pre-injection stimulation than post-injection

stimulation. It is important to note that the overall average mean values during early stimulation were significantly higher than the mean values during late stimulation.

Anova: Two-Factor						
SUMMARY	***Count***	***Sum***	***Average***	***Variance***		
ACTIVITY						
Early Stimulation	3	324.67	108.2233	34.49779		
Late Stimulation	3	341.7925	113.9308	28.25751		
SUBJECTS						
Cat 1	2	213.87	106.935	19.12711		
Cat 2	2	234.8825	117.4413	12.94133		
Cat 3	2	217.71	108.855	17.11125		
Source of Variation	***SS***	***df***	***MS***	***F***	***P-value***	***F crit***
ACTIVITY	48.86333	1	48.86333	308.9133	0.003222	18.51276
SUBJECTS	125.1943	2	62.59713	395.7382	0.002521	19.00003
Error	0.316356	2	0.158178			
Total	174.3739	5				

Table 4.4a ANOVA For Early and Late Responses for Baseline Stimulation Block

Anova: Two-Factor						
SUMMARY	***Count***	***Sum***	***Average***	***Variance***		
ACTIVITY						
Early Stimulation	3	288.84	96.28	87.95802		
Late Stimulation	3	305.7475	101.9158	91.20695		
SUBJECTS						
Cat 1	2	176.685	88.3425	13.80751		
Cat 2	2	208.0525	104.0263	40.92863		
Cat 3	2	209.85	104.925	3.393012		
Source of Variation	***SS***	***df***	***MS***	***F***	***P-value***	***F crit***
ACTIVITY	47.64393	1	47.64393	9.08782	0.09467	18.51276
SUBJECTS	347.8447	2	173.9224	33.17474	0.029261	19.00003
Error	10.48523	2	5.242614			
Total	405.9739	5				

Table 4.4b ANOVA For Early and Late Responses for 5 min Post-Injection Stimulation Block

Anova: Two-Factor						
SUMMARY	***Count***	***Sum***	***Average***	***Variance***		
ACTIVITY						
Early Stimulation	3	314.51	104.8367	4.879377		
Late Stimulation	3	289.1225	96.37417	34.01265		
SUBJECTS						
Cat 1	2	192.9	96.45	91.53045		
Cat 2	2	207.745	103.8725	24.2208		
Cat 3	2	202.9875	101.4938	11.99275		
Source of Variation	***SS***	***df***	***MS***	***F***	***P-value***	***F crit***
ACTIVITY	107.4209	1	107.4209	10.57128	0.08299	18.51276
SUBJECTS	57.46091	2	28.73046	2.827363	0.261276	19.00003
Error	20.32314	2	10.16157			
Total	185.2049	5				

Table 4.4c ANOVA For Early and Late Responses for 15 min Post-Injection Stimulation Block

Anova: Two-Factor						
SUMMARY	***Count***	***Sum***	***Average***	***Variance***		
ACTIVITY						
Early Stimulation	3	326.5575	108.8525	0.963006		
Late Stimulation	3	284.13	94.71	45.33711		
SUBJECTS						
Cat 1	2	196.9075	98.45375	256.5679		
Cat 2	2	207.815	103.9075	30.69361		
Cat 3	2	205.965	102.9825	71.2818		
Source of Variation	***SS***	***df***	***MS***	***F***	***P-value***	***F crit***
ACTIVITY	300.0155	1	300.0155	10.25206	0.085253	18.51276
SUBJECTS	34.07239	2	17.0362	0.582157	0.632048	19.00003
Error	58.52783	2	29.26392			
Total	392.6157	5				

Table 4.4d ANOVA For Early and Late Responses for 30 min Post-Injection Stimulation Block

Anova: Two-Factor						
SUMMARY	***Count***	***Sum***	***Average***	***Variance***		
ACTIVITY						
Early Stimulation	3	292.58	97.52667	95.43885		
Late Stimulation	3	280.595	93.53167	53.01213		
SUBJECTS						
Cat 1	2	172.58	86.29	2.71445		
Cat 2	2	204.7875	102.3938	41.74695		
Cat 3	2	195.8075	97.90375	0.133903		
Source of Variation	***SS***	***df***	***MS***	***F***	***P-value***	***F crit***
ACTIVITY	23.94004	1	23.94004	2.318056	0.267314	18.51276
SUBJECTS	276.2467	2	138.1234	13.37415	0.069569	19.00003
Error	20.65527	2	10.32763			
Total	320.842	5				

Table 4.4e ANOVA For Early and Late Responses for 50 min Post-Injection Stimulation Block

CHAPTER 5

CONCLUSION AND SUGGESTIONS FOR FUTURE RESEARCH

5.1 Summary of Results

There are no available human studies that have attempted to correlate human motor activity with the behavior observed with administration of Prozac. The major hypothesis in this series of experiments is that Prozac suppresses muscle activity during expression of emotional stimulated behavior in both time and dosage-dependent manner. The reduction in the EMG signal as reflected in the downward shift in MF suggests that the firing rate as well as the recruitment pattern of muscle fibers is suppressed. This research substantiates episodes of muscle modulation during early stimulation Vs late stimulation. It is noteworthy to mention that there may be several other mechanisms that are involved than fatigue due to modulatory effects that my be related to other central nervous systems such as synaptic inhibitions as well as recruitment of other structures in the brain that may induce inhibition. An important observation is that the values of the power of the wavelet coefficients are significantly higher in all frequency ranges for early stimulation than late stimulation responses.

It is also noteworthy that there is a significant difference between the mean frequency values in the early stimulation response than in the late stimulation response. This would indicate that the high frequency component present during early stimulation influences the activity of the fast-firing motoneurons more substantially than during late stimulation response and therefore shows influence of central inhibition.

This research also proves that the wavelet time frequency signal decomposition, using the Daubechies order 6 (db6) wavelet, is capable of separating activities at various frequency levels while providing insight into the structure of the time series at various scales. The results of the present study clearly indicate episode of both central and peripheral modulation on the masseter muscle during hypothalamic electrical stimulation mediated by Prozac.

5.2 Suggestions for Future Work

This research shows that the wavelet transform technique is a viable method for frequency analysis of the SEMG signal. This technique does not assume that the signal is stationary, and provides a reliable time-based frequency spectrum. As such, it has multi-faceted potential for future research in the study of neuromuscular dysfunction. Future work should include: pre-stimulation Vs post stimulation analysis to see the effects of fatigue from the stimulation episode; pre-stimulation Vs early stimulation analysis to observe immediate effects of stimulation; pre stimulation Vs late stimulation analysis to observe the effects of fatigue and stimulation together; early stimulation Vs post stimulation analysis to check stimulation effects without fatigue; late stimulation vs post stimulation to measure the long lasting effects of fatigue. The next step in this effort will be to analyze the baseline data set at different time blocks (5min, 15min, 30min, and 50min) Vs the post injection data set at the same time blocks to be able to observe the effect of the drug on the hypothalamic electrical stimulation.

APPENDIX A

LABVIEW PROGRAM USED FOR FILTERING

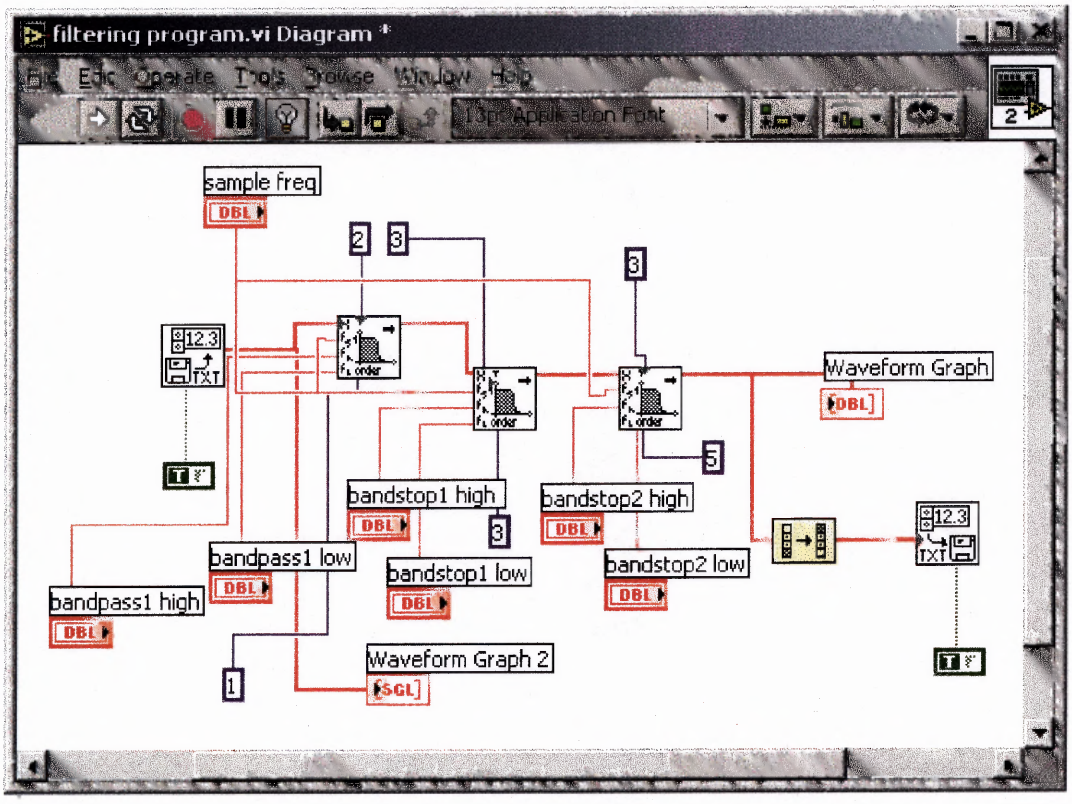

Figure A.1 this is the back panel of the labview program used to filter the data.

APPENDIX A

LABVIEW PROGRAM USED FOR FILTERING

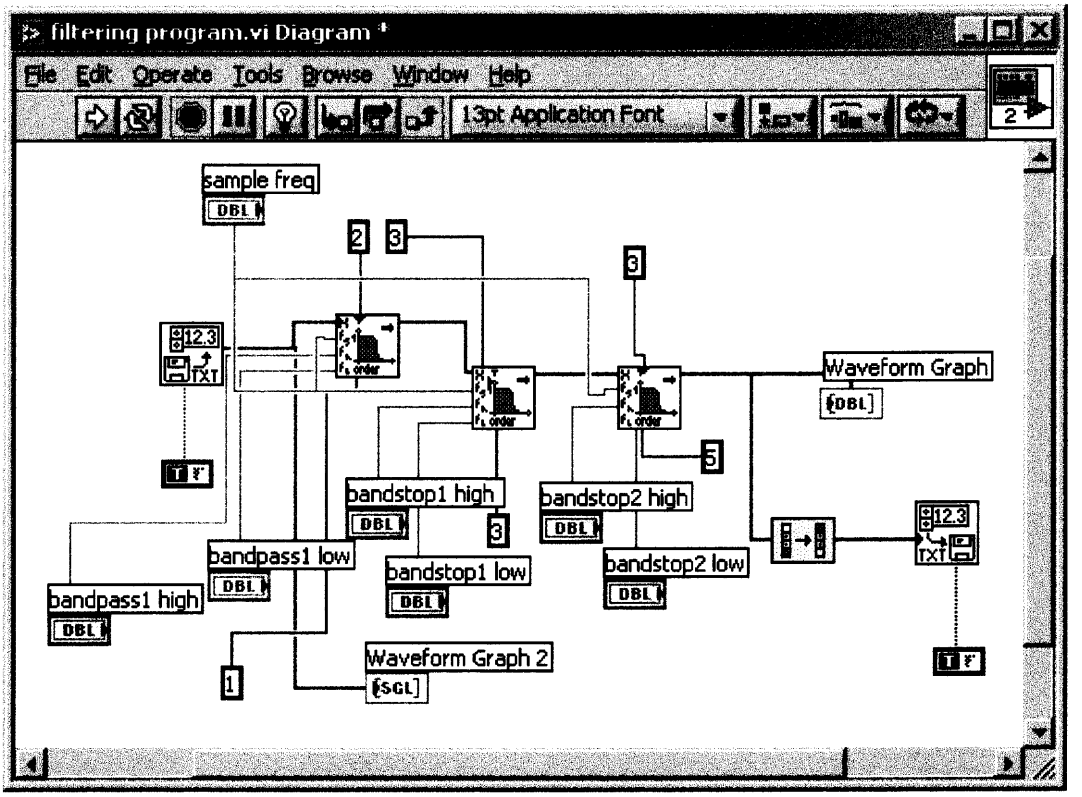

Figure A.1 this is the back panel of the labview program used to filter the data.

APPENDIX B

MATLAB PROGRAM DEVELOPED FOR THE RESEARCH

This Appendix contains the Matlab program that performed the wavelet analysis used in this research. This program takes user inputs of 'file to be analyzed' and 'wavelet type to use' and performs the continuous wavelet transforms on the file. The mean power frequency is then calculate and averaged to get the desired result.

```
clc
disp(' Welcome to fatigue analysis ');
[fname,pname]=uigetfile('*.*','enter file to be analyzed:');
 filename = [pname fname];
 load(filename);
 fname = strtok(fname,'.');
%filename = input('please enter the name of the file without
extension:','s');
secperblock=input('please enter #seconds per analysis block:');
interestsec=input('enter the total number of seconds data for
analyses:');

samplerate=2000;
%originallengthsec=90;
%originarraylength=originallengthsec*samplerate;
interestarraylength=interestsec*samplerate;

meanfreqarray=[];  %meanfreqpoint=[];finalmeanarray=[];
%loadfile=sprintf('%s.asc',filename);

%disp(sprintf('accepting first %d data points (%d seconds) as data of
interest...',interestarraylength,interestsec))
%disp(sprintf('rejecting %d seconds of data from each
block...',secperblock-interestsec));
%disp(sprintf('rejecting first %d seconds (1 block) of
data..',secperblock));
Dmatrix=[];

no_of_blocks=fix(interestsec/secperblock);
file=eval(fname);
ch=1;
Dmatrix=file(7000:11999,ch);
blocksize=length(Dmatrix)/no_of_blocks;
delta=1/samplerate;
Dmatrix=Dmatrix-mean(Dmatrix);
%t=delta.*[1:length(Dmatrix)];
wname='db3';

scales=[4:.1:31];
frequencies=scal2frq(scales,wname,delta);
meanfreq=[]; coeff_freq_sum=[]; row_sum=[];row_sum1=[]; row_sum2=[];

for block=1:no_of_blocks,
```

```
        data=Dmatrix((block-1)*blocksize+1:(block*blocksize));
        wcoeff=cwt(data,scales,wname);
        %Q=abs(Q);

      for i=1:size(wcoeff,1)
          %j=1:size(Q,1);
         % for i=1:size(a,1)
    row_sum(i)=sum(wcoeff(i,:));
    row_sum1(i)=row_sum(i)/size(wcoeff,2);
    row_sum2(i)=row_sum1(i).^2;
    coeff_freq_sum(i)=row_sum2(i).*frequencies(i);
end
%t=t(size(a,2)/2);
meanfreq=sum(coeff_freq_sum)/sum(row_sum2);
          %a=Q(:,i);
          %a=a';
          %meanfreq(i)=sum((a(j).*frequencies(j)))/(sum(a(j)));

          %max_of_Q(i)=find(a==max(a));
        %meanfreqpoint=waveletmean(temparray,samplerate);
        %disp(sprintf('mean frequency for block# %d is
%f\n',block,meanfreqpoint))


   meanfreqarray=[meanfreqarray meanfreq];

end
mean_of_meanfreqarray = mean(meanfreqarray)
    t=secperblock:secperblock:interestsec;
    %plot(t,meanfreqarray);
    %n=finalmeanarray(1:no_of_blocks);

    %figure;
    %plot(m,n,'r*');
    %title('Mean frequency Vs Time plot for FatiqueData2');
    %xlabel('Time(s)');
    %ylabel('Mean Frequency (Hz)');

    %determine least-squares fit and plotting result
 %for i=1:1:1
     %linefit1(meanfreqarray',sprintf('%s',fname),t,secperblock);
     %end



%%function fit=linefit1(y,plotfitfilename,timeinterval,SecondsPerBlock)

%function fit=linefit(y)
%load y.txt;

%%y = [116.04 88.44 107.26 103.61 75.16 84.70 98.62 84.38 95.10 88.05
...
  %%      78.09 97.50 90.44 80.43 87.54 90.10 90.39 80.98 85.53
83.60]';
  y = [111.78 99.23 93.83 95.86 98.16]';
N=length(y);
```

```
%%X= [0 2 4 6 11 13 15 17 21 23 25 27 36 38 40 42 56 58 60 62]';
X = [3 14 24 39 59]';
%%X=timeinterval';%[0:(N-1)]';
Mslope=(N*(X'*y)-sum(X)*sum(y))/(N*(X'*X)-sum(X)^2)
Bintercept=(sum(y)-Mslope*sum(X))/N
rcoeff=(N*(X'*y)-sum(X)*sum(y))/((N*(X'*X)-sum(X)^2)^.5*(N*(y'*y)-
sum(y)^2)^.5)
%Mslope=Mslope/SecondsPerBlock;
fit=[Mslope Bintercept rcoeff];

clf;                              % clear any previous figure
plot(X,y,'*');           % plot y as a function of x and display each
point with symbol "*"
%%%p=polyfit(X,y,1)      % do a first-order polynomial fit between x and
y
%%%yy=polyval(p,X); % evaluate the polynomial at the x (or other
selected points)
%%%hold on               % hold the last display
%%%plot(X,yy)      % plot yy vs. x on the previous figure

%%%tstring1=sprintf('slope = %4.4f\n',fit(1));
%%%tstring2=sprintf('y int = %4.4f\n',fit(2));
%%%tstring3=sprintf('r val = %1.4f',fit(3));
%%%text(25,min(y(2:N))+.95*(max(y(2:N))-min(y(2:N))),tstring1)
%%%text(25,min(y(2:N))+.85*(max(y(2:N))-min(y(2:N))),tstring2)
%%%text(25,min(y(2:N))+.75*(max(y(2:N))-min(y(2:N))),tstring3)
%%xlabel(sprintf('Time Interval of %d sec block',SecondsPerBlock))
ylabel('Mean Frequency (Hz)');
xlabel('Time(M)'); %ylabel('y');
Title('Wavelet mean frequency analysis');



clear all;
clc;
% Ask the user to select the signal that is to be analyzed.
[fname,pname]=uigetfile('*.*','Please select the file that will be
analyzed with a wavelet:');
if isstr(fname) == 0
    disp(' Cannot find file')
    dbquit
end
Filename = [pname fname];
load(Filename) ;% load file
fname = strtok(fname,'.');     % drop extension
k=eval(fname);                 % evaluate fname
signal=k(1000:length(k)); %Filter transient lasts approximately first
1000 points
N=length(signal);
ss=signal;
maxscale=8;      % Set max scale level, based on decomposition
ss = detrend(ss);
% Allow user to enter type of wavelet to be used in this analysis,
accepting wave name as 'wn', a string.
wave=input('Please enter name of Wavelet to be used in analysis --->
','s');
```

```
sf=2000;        % Sampling Freq for EMG signals is 2 kHz.
sp=1/sf;        % Sampling Period
a=2.^[1:maxscale];  % Set Scales
t=sp.*[1:length(ss)]; % convert file to seconds, not sample number
figure;
plot(t,ss)
title(['EMG Activity During post-injection Stimulation']);
xlabel('Time (s)');
ylabel('EMG Amplitude [mV]');
```

REFERENCES

1. S. Palla and M. M.Ash Jr. "Power Spectral Analysis of the Surface Electromyogram of the Human Jaw Muscles During Fatigue." *Archs Oral Biol.* 26 (1981): 547-553.

2. A.Blank , B. Gozen and A. Magora. "The Size of Active Motor Units in the Initiation and Maintenance of an Isometric Contraction Carried out to Fatigue" *Electromyogr. Clin. Neurophysiol.* 19 (1979): 535-539.

3. K.Sakamoto, T. Usui, A. Haami and K. Ohkoshi. "The Wave Analyses with the Fast Fourier Transform on Surface Electromyogram and Tremor during an Acute and an Accumulative Fatigue." *Electromyogr. Clin. Neurophysiol.* 22 (1982):207-228.

4. S. Weiner, M. B. Shaikh, and A. Siegel A. "Electromyographic Activity in the Masseter Muscle Resulting from Stimulation of Hypothalamic Behavioral Sites in the Cat." *J Orofac Pain.* 7 91993): 370-377.

5. P. Leyhausen, Cat Behavior. "The Predatory and Social Behavior of Domestic and Wild Cats". *New York: Garland STPN Press*; 1979

6. Y. Han, M. B. Shaikh, A. Siegel. "Medial Amygdaloid Suppression of Predatory Attack Behavior in the Cat": I. Role of a Substance P Pathway from the Medial Amygdala to the Medial Hypothalamus, *Brain Res.* &16 (1996) 5971.

7. C. L.Lu , M. B. Shaikh, A. Siegel. "Role of NMDA Receptors in Hypothalamic Facilitation of Feline Defensive Rage Elicited from the Midbrain Periaqueductal" Gray, *Brain Res.* 581 (1992): 123-132.

8. S. Stoddard-Apter, B. Levin, A. Siegel. "A Sympathoadrenal and Cardiovascular Correlates of Aggressive Behavior in the Awake Cat". J *Auton Nerve Syst* 8 (1993): 343-360

9. J. P Flynn , H. Vanegas, W. E. Foote, S. Edwards. "Neural Mechanisms Involved in a Cat's Attack on a Rat", Whalen R, Editor. The Neural Control of Behavior. *New York: Academic Press*, (1970): 135-73.

10. J. W. Cheu, A. Siegel. "GABA Receptor Mediated Suppression of Defensive Rage Behavior Elicited from the Medial Hypothalamus of the Cat": Role of the Lateral Hypothalamus. *Brain Res.* 783 (1998): 293-304.

11. L. Siever, and R. L. Tristman. "The Serotonin System and Aggressive Personality Disorder." *Int. Clin. Psychopharmacol.* 8:2 (1993): 33-39.

12. N. K. Popova, A. V. Kulikov, E. M. Nikilina, E. Y. KolachKove. and G. B.

Maslova. "Serotonin Metabolism and Serotonergic Receptors in Norway Rats Selected for Low Aggressiveness to Man." *Aggress. Behav.* 17 (1991b): 207- 213.

13. V. Molina, S. Gobaille, and P. Mandel. "Effects of Serotonin-mimetic Drugs on Mouse-killing Behavior." *Aggress. Behav.* 12 (1986):201-211.

14. H. Golebiewski, A. Romaniuk. 'The Participation of Serotoninergic System in the Regulation of Emotional-Defensive Behavior Evoked by Intrahypothalamic Carbachol Injections in the Cat." *Acta Neurobiol.* Exp. 45 (1985) 25-36.

15. R. Bottinelli, M. A. Pellegrino, M. Canepari, R. Rossi, and C. Reggiani. "Specific Contributions of Various Muscle Fiber Types to Human Muscle Performance: an in Vitro Study." *J Electromyorgr kinesiol* 9: 87-95, 1999

16. R. E. Burke, D. N.Levine, P. Tsairis, and F. E. Zajac. "Physiological Types and Histochemical Profiles in Motor Units of the Gastrocmemius." *J Physiol* (Lond) 234: 723-748, 1973

17. E. Henneman, G. Somjen, and D. O. Carpenter. "Functional Significance of Cell Size in Spinal Motoneurons". *J Neurophysiol* 28: (1965): 560-582

18. L. Lindstrom, R. Kadefors, and I. Petersen. "An Electromyographic Index for Localized Muscle Fatigue". *J Appl Physiol* (1977): 750-754

19. M. Solomon, C. Baten, J. Smit, R. Baratta H. Hermens, R. D'Ambosia, and H. Shoji. "Electromyogram Power Spectra Frequencies Associated with Motor Unit Recruitment Strategies". *J Appl Physiol* 68 (1990): 1177-1185

20. J. H. T. Viitasalo, and P. V. Kome. "Signal Characteristics of EMG during Fatigue". *Eur J Appl Physiol* 37 (1977): 111-121

21. M. J. Gooupil, M. Auvergne, A. Baglin. 1991, A&A 250, 89 NASA ADS

22. http://salmon.psy.plym.ac.uk/year1/stressho.htm. Hormones and Stress: The Pituitary-adrenal-axis in Learning and Memory. (27 April 2002)

23. D. Ottoson. *Physiology of the Nervous System.* New York: Oxford University Press, 1983.

24. P. Sparto, M. Parnianpour, E. Barria and J. Jagadeesh, "Wavelet and Short-Time Fourier Transform Analysis of Electromyography for Detection of Back Muscle Fatigue." *IEEE Trans. on Rehabilitation Engineering* 8:3 (2000): 433-36.

25. P. Dolan, A. Mannion and M. Adams. "Fatigue of the Erector Spinae Muscles. A

Quantitative Assessment using "frequency banding" of the Surface Electromyography Signal." *Spine* 20 (1995): 149-159.

26. A. Vander, J. Sherman and D. Luciano. *Human Physiology: The Mechanisms of Body Function*. 5th Ed. New York: McGraw-Hill, 2001.

27. J. Webster." *Medical Instrumentation: Application and Design*. 3rd Ed." New York: John Wiley and Sons, 1998.

28. S.A.G Fuchs, H.M Edinger, A. Siegel, "The Organization of the Hypothalamic Pathways Mediating Affective Defense Behavior in the Cat." *Brain Res.* 330 (1985) 77-92

29. S. Weiner, M. Shaikh and A. Siegel, "Electromyographic Activity in the Masseter Muscle Resulting from Stimulation of Hypothalamic Behavioral Sites in the Cat," *J. Orofacial Pain*. 1993; 7; 370-376.

30. P. Smitthisomwong, S. Weiner, L. Levin, S.Reisman and A. Siegel. "The Effect of a Cholecystokinin Agonist on Masseter Muscle Activity in the Cat." *J. Dental Research* 79:10 (2000): 1823-28.

31. F. Hellstrom, J. Thunberg, M. Bergenheim, P. Sjolander, J. Pederson and H. Johansson. "Elevated Intramuscular Concentration of Bradykinin in Jaw Muscle Increases the Fusimotor Drive to Neck Muscles in the Cat." *J. Dent. Res.* 79:10 (2000): 1815-22.

32. A. Poularikas, ed. *Transforms and Applications Handbook*. London: CRC Press, January 1996.

33. S. Mallat, *A Wavelet Tour of Signal Processing*. San Diego: Academic, 1998.

34. Mathworks, Incorporated. *Matlab Wavelet Toolkit*. Rev. 2. http://www.mathworks.com/access/helpdesk/help/pdf_doc/wavelet/wavelet_ug.pdf.(September 2001)

35. E. Serrano and M. Fabio. "Application of Wavelet Transform to Acoustic Emission Signal Processing." *IEEE Trans. on Signal Processing* 44:5 (1996): 1270-75.

36. N. Martin, J. Mars, J. Martin, and C. Chorier. "A Capon's Time-Octave Representation Application in Room Acoustics." *IEEE Trans. on Signal Processing* 43:8 (1995): 1842-54.

37. L. Shang, G. Herold and J. Jaeger. "A New Approach to High-Speed Protection for Transmission Line Based on Transient Signal Analysis Using Wavelets." *IEEE Developments in Power System Protection, Conference Publication* 479

(2001): 173-76.

38. P. Maass, G. Tescheke, W. Willmann and G. Wollmann. "Detection and Classification of Material Attributes – A Practical Application of Wavelet Analysis." *IEEE Trans. on Signal Processing* 48:8 (2000):2432-38.

39. C. Pattichis, and M. Pattichis. "Time-Scale Analysis of Motor Unit Action Potentials." *IEEE Trans. on Biomedical Engineering* 46:11 (1999): 1320-29

40. National Instruments Corporation. *Wavelet and Filter Bank Design Toolkit Reference Manual.* January, 1997. http://www.ni.com/pdf/manuals/321380a.pdf. (February 2002)

41. C. Valens. "A Really Friendly Guide to Wavelets." 1999. http://perso.wanadoo.fr/polyvalens/clemens/wavelets/wavelets.html. (August 2002)

42. R. Merletti, L. Conte and C. Orzio. "Indices of Muscle Fatigue." *J. Electromyographic Kinesiology* 1 (1991): 20-33.

43. J. Karlsson, B. Gerdle and M. Akay. "Analyzing Surface Myoelectric Signals Recorded During Isokinetic Contractions." *IEEE Engineering in Medicine and Biology* 6 (2001): 97-105.